Quaternary Science Reviews 179 (2018) 1–23

Contents lists available at ScienceDirect

Quaternary Science Reviews

journal homepage: www.elsevier.com/locate/quascirev

Paleolakes in the Gobi region of southern Mongolia

Frank Lehmkuhl [a, *], Jörg Grunert [b], Daniela Hülle [c], Ochirbat Batkhishig [d], Georg Stauch [a]

[a] RWTH Aachen University, Department of Geography, Templergraben 55, 52062 Aachen, Germany
[b] University of Mainz, Department of Geography, Johann-Joachim-Becher-Weg 21, 55099 Mainz, Germany
[c] University of Cologne, Institute of Geography, Albertus-Magnus-Platz, 50923 Cologne, Germany
[d] Institute Geography-Geoecology, Mongolian Academy of Science, Erkhuu str. 11r horoolol, Sukhbaatar duureg, Ulaanbaatar 14192, Mongolia

ARTICLE INFO

Article history:
Received 14 June 2017
Received in revised form
12 October 2017
Accepted 27 October 2017

Keywords:
Mongolia
Lake level variations
Geomorphological maps
Late Quaternary

ABSTRACT

Numerous lakes and remnants of paleolakes exist in western and southern Mongolia. For six basins in the area, detailed geomorphological maps were compiled, based on extensive field studies and remote sensing datasets. Several phases of high and low lake levels were reconstructed and dated by radiocarbon and optically stimulated luminescence. During the marine isotope stage (MIS) 6 lakes in southern and western Mongolia mostly disappeared. In contrast, large paleolakes existed during the last interglacial (MIS 5e) and lasted probably until the beginning of the last glacial. These huge lakes were caused by a strong East Asian summer monsoon, which reached southern and even western Mongolia. During the MIS 3 the monsoon was considerably weaker and most of the lakes were relatively small or even disappeared. Higher lake levels of this period were only recorded at the Orog Nuur. However, at this time the lake was fed by glacial melt water from the Khangai Mountains. The MIS 2 was again a very dry period. The previously supposed phase of synchronous high lake levels and glaciations in southern and western Mongolia is not supported by the data presented here. During the Holocene, lakes in the western and southern part of the study area evolved differently. Early Holocene high lake levels were reconstructed for the western lakes, while most of the southern lakes had highest lake levels in the mid-Holocene. These differences can be attributed to different moisture bearing atmospheric systems. In the late Holocene lake levels were generally low and in the last 50 years most lakes completely disappeared due to a strong human usage of the water resources.

1. Introduction

In semiarid western and southern Mongolia numerous lakes fill the large endorheic basins (Fig. 1). The area is known as “Valley of the Lakes”, which can be divided into the “Basin of the Great Lakes” in northwestern Mongolia, and to the south between Khangai and Gobi Altai, the so-called “Valley of the Gobi Lakes”. Pleistocene lake levels and shorelines of varying altitude can be observed in almost every lake basin. The earliest observations on high lake levels in the deserts of Mongolia were reported in the early and mid-20th century (e.g. Berkey and Morris, 1927; Murzaev, 1954; Devjatkin, 1981). A geomorphological map of Mongolia at the scale 1: 1.5 Mio. was published by Deviatkin et al. (1987) and showed the shorelines of large paleolakes in western and southern Mongolia of Pleistocene and Holocene age. At Uvs Nuur and Khyargas Nuur (Nuur = lake) three shorelines at different elevations above the modern lake levels were distinguished: The lowermost at 10–30 m above the present lake level indicates paleolakes of moderate expansion, the second one at around 130 m indicates large paleolakes and the uppermost more than 300 m is indicative of giant paleolakes. For the Valley of the Gobi Lakes a similar lake extent has been reconstructed by Komatsu et al. (2001) using remote sensing data. However, in both studies information on the exact timing was not obtained. At the Uvs Nuur a 10 m-high cliff line has a Holocene age, and a cliff at the eastern border of the lake 20 m high was radiocarbon dated to 43,598 ± 654 cal. BP (Grunert et al., 2000). No indications for a cliff line at around 130 m were found, but lacustrine sediments 250 m above the modern lake level were found east of the Uvs Nuur, near the small interdune lake Bayan Nuur, pointing to a giant mid-Pleistocene paleolake (Walther, 1999; Naumann and Walther, 2000). The authors describe typical lacustrine sediments as follows: Light-grey, horizontally bedded silts with a carbonate content up to 30% covered by hard crusts at the bare surface. Numerous fragments of *Phragmites* are embedded, and dispersed

* Corresponding author.
E-mail address: flehmkuhl@geo.rwth-aachen.de (F. Lehmkuhl).

https://doi.org/10.1016/j.quascirev.2017.10.035

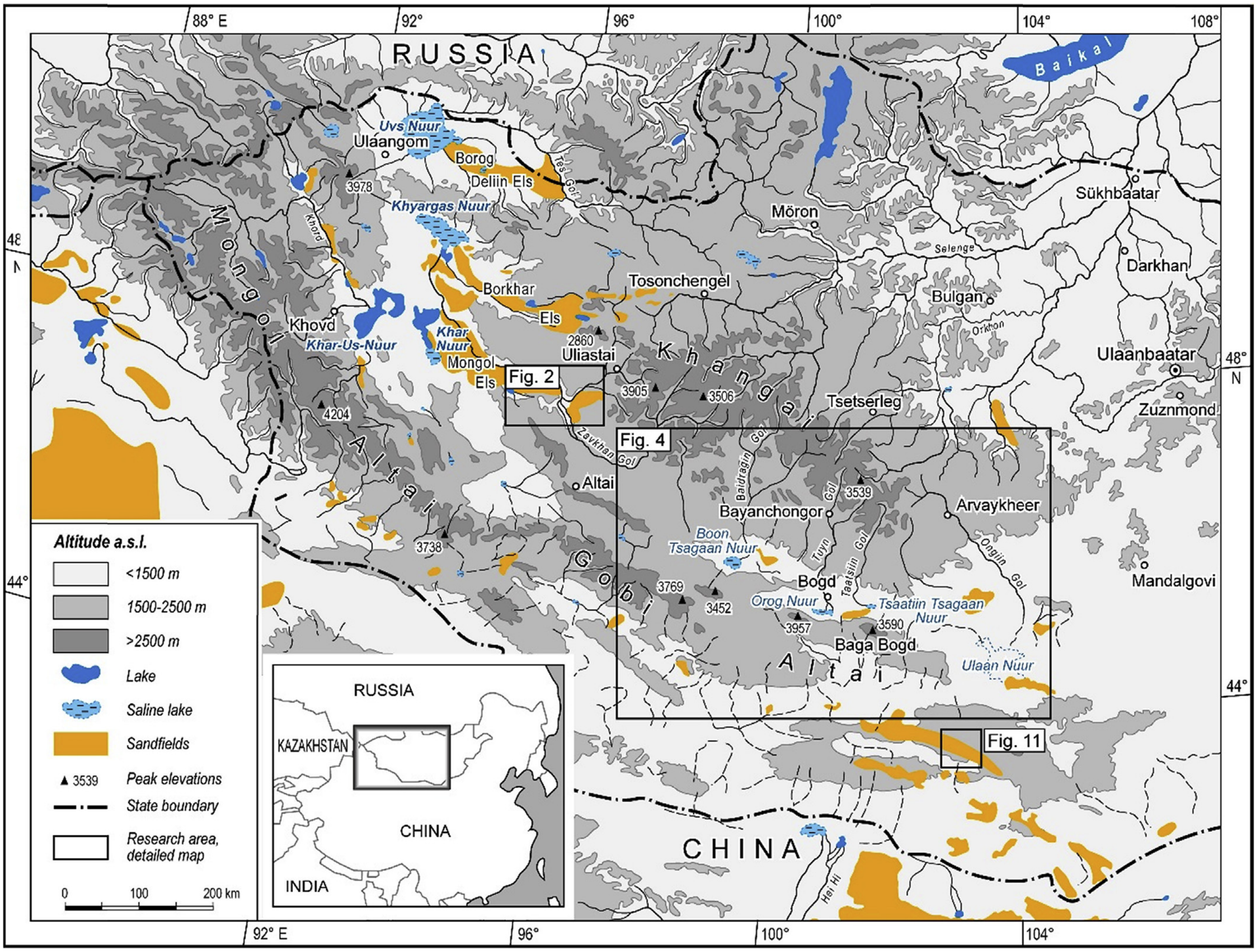

Fig. 1. Study area in Western and Central Mongolia including lakes and sandfields.

but locally concentrated, small mollusc (snail) shells indicating a former swamp vegetation which corresponded with a paleolake-level at a defined altitude a.s.l.

First detailed studies on lake level variations in southern Mongolia were obtained in the depression of the Bayan Tohomin Nuur (Fig. 1). Grunert et al. (2009) and Felauer et al. (2012) provided evidence for higher than present lake levels in the early Holocene. According to Dorofeyuk (2008) early Holocene high lake levels in Mongolia occurred at 9500 BP, and the lakes started to increase 8000 BP reaching their maximum lake levels in 7500 to 7000 BP. From 7000 BP regression started resulting in similar lake levels as the present ones and lowest lake level occured in 3000 to 4000 BP. According to Khosbayar (2005), the last warm period in Mongolia lasted from 6500 to 3250 BP and from 3000 to 2000 BP there was an increase of lake levels. Since 2000 BP lakes receded continuously (Dorofeyuk, 2008). An early Holocene humid period was also deduced from results obtained from Ulaan Nuur (Lee et al., 2011, 2013). While only few results for Holocene lake levels were reported for the Valley of the Gobi Lakes in southern Mongolia, numerous studies are available for northern Mongolia. An array of references including Tarasov and Harrison (1998), Walther (1999), Tarasov et al. (1999, 2000), Lehmkuhl and Haselein (2000), Yang et al. (2004), Herzschuh (2006), and An et al. (2008) have presented an overview concerning the Holocene lacustrine and/or vegetation history showing especially early and mid-Holocene humidity. Watanabe et al. (2009) summarized results from sediment cores of Lake Baikal and Lake Hovsgol and calculated linear sedimentation rates. In the cores the TOC concentration rapidly increased at the end of the last glacial with laminated layer deposited during Bølling/Allerød interval. A summary of moisture changes from lakes in mid-latitude arid Central Asia was provided by Chen et al. (2008) indicating major moisture phases in the mid-Holocene. From buried soil ^{14}C dating results it is possible to distinguish several Holocene wet and dry periods in Mongolian Altai region; dry periods from 2150 to 1700, 1300 to 1050, 680 to 250 BP and wet periods 1700 to 1300, 1005 to 680 BP and the last 2–3 centuries (Dinesman et al., 1989).

The former extension of glaciations were supposed to be synchronous with lake level rise (Deviatkin et al., 1987) and were recently investigated on the western flank of the Otgon Tenger mountains in the western Khangai (Rother et al., 2014; Lehmkuhl et al., 2016). Terminal moraines of MIS 2 were reported at 1900 m a.s.l., and at about 1800 m a.s.l., moraines of MIS 3 were found. They likely indicate more humidity (snowfall) in the Khangai at that time. In the Altai, the maximum extent of glaciers was reached during the MIS 2 (Lehmkuhl et al., 2011, 2016).

Lehmkuhl et al. (2011, 2012) focused on Late Pleistocene and Holocene environmental change in central and northern Mongolia derived from aeolian and colluvial sediments. They showed different moisture phases in the early and mid-Holocene and a dry late Holocene and suggest a stronger human impact in the latter phase. The chronologies for the studied sites were predominately obtained by luminescence dating of aeolian, colluvial, and lacustrine sediments, indicating respective climate changes during the Late Quaternary.

However, up to now, the spatial and temporal evolution of the paleoclimate in Mongolia is only poorly resolved. The exact timing of phases with higher and lower humidity, e.g. early versus mid-Holocene, was not reconstructed so far. Hence, this study focuses on lake level evolution and paleohydrological changes during the late Quaternary in the lake basins of western and southern Mongolia. Detailed geomorphological maps were compiled for detecting different paleoshorelines. Available ages constraining the timing of high and low lake levels are summarized for each individual basin. Finally, possible forcing mechanism for the development of the lakes and the paleoclimate evolution are discussed.

2. Study area

2.1. Climatic setting

The modern climatic conditions are of continental type showing large temperature variations with mean summer temperatures of about 20 °C and mean winter temperatures below 20 °C. The highest amount of annual precipitation occurs in the eastern Altai and central Khangai (400–500 mm; Academy of Sciences of Mongolia and Academy of Sciences of USSR, 1990), which are influenced by the mid-latitude westerlies. The most eastern part of the Altai, bordering the Valley of the Great Lakes, is situated in a rain shadow and experiences more arid conditions (150–300 mm). In the basins of the Valley of the Great Lakes and the Valley of the Gobi Lakes, the annual precipitation decreases to 100–200 mm and locally to less than 50 mm (Academy of Sciences of Mongolia and Academy of Sciences of USSR, 1990). There is a pronounced seasonal precipitation distribution characterized by 70–80% of the annual precipitation falling during the summer months.

2.2. Geomorphic setting

2.2.1. Valley of the Great Lakes

The largest lakes in the center of the vast tectonic depression (basin of the Great Lakes) between the Mongolian Altai and the Khangai are Uvs Nuur (760 m a.s.l.) and Khyargas Nuur (1028 m a.s.l.), both with brackish water. South of Khyargas Nuur two smaller lakes, Khar-Us Nuur (1130 m a.s.l.) and Khar Nuur near Khovd, consist of freshwater bodies and drain into the Khyargas Nuur (Fig. 1). The Khar-Us Nuur is fed by the Zavkhan Gol (gol = river), the middle course of the river will be presented in this paper. Eastwards of these lakes, near the foothills of the Khangai Mountains, three dunefields with a length of more than 200 km are located. They are named from north to south: Borog Deliin Els, Borkhar Els and Mongol Els (Fig. 1). As the dunefields occur at the eastern border of the lakes, their formation has been interpreted as a result of deflation from the dried lake bottoms by strong WNW – winds during former arid periods, of the Last Glacial Maximum, for example, when the lakes completely dried out (Walther, 1999; Grunert et al., 2000; Naumann and Walther, 2000; Grunert and Dash, 2004; Grunert and Lehmkuhl, 2004).

2.2.2. Valley of the Gobi Lakes

The terminal lakes Boon Tsagaan Nuur (1300 m a.s.l.) and Adagin Tsagaan Nuur (1283 m a.s.l.), Orog Nuur (1220 m a.s.l.), Taatsiin Tsagaan Nuur (1240 m a.s.l.) and Ulaan Nuur (1027 m a.s.l.) cover the deepest parts of the broad WNW-ESE–stretching tectonic depression named “Valley of the Gobi Lakes” (Fig. 4). Strong earthquakes – the last one occurred in1957 with a magnitude of 8.1 – are indicative of neotectonic movements along a main fault separating the young Gobi Altai from the old Khangai massive (Baljinaym et al., 1993; Kurushin et al., 1997; Owen et al., 1997). All rivers originating in the Khangai Mountains are perennial with highest discharge during the rainy season in summer and a minimum in winter.

3. Materials and methods

3.1. Geomorphological mapping, site selection and sampling strategy

Natural exposures with thicknesses ranging from 2 m to 8 m were sampled after preparation of the sections. The main investigations concentrated on sections situated in the Valley of the Gobi Lakes (Fig. 1, Table 1). Field work comprised geomorphological mapping and the analysis of tectonic and geomorphological structures and landforms supported by the use of GPS, barometric altimetry and levelling, topographic maps of 1:100,000, 1:500,000 and Landsat-TM images. Detailed sedimentological and geomorphological analyses of fluvial terraces, lakes and indications for former lake levels (beach ridges, silty sediments), alluvial fans and aeolian landforms and sediments were performed to provide a framework of the late Pleistocene and Holocene evolution (see supplement). This includes the sampling of suitable material for radiocarbon and luminescence dating from key locations and horizons. Additional information by figures (Figs. S1 – S31) and tables (Tables S1 - S21) are provided in the supplement.

3.2. Dating methods

Typical lake sediments are carbonate silts. Some of them contain charcoal or snail shells which are suitable for radiocarbon dating. However, most of the remnants of former lakes are dated only indirectly by OSL (optical stimulated luminescence) technique of the underlain sand layers. These insufficiencies can only be reduced by detailed geomorphological mapping of the supposed lake levels and by sampling the remnants at one level at different places to compare the dates later on.

3.2.1. Luminescence dating

To provide information on the geochronological context, OSL dating was applied to 43 samples from 26 sections (Table 1, Table S21). With OSL dating, the time elapsed since the last exposure of quartz or feldspar grains to sunlight during transport processes can be determined. For a summary of the technical basics and a review of application studies see e.g. Aitken (1998), Bøtter-Jensen et al. (2003) and Preusser et al. (2008).

All samples taken for luminescence dating were subjected to the standard routine described by Hülle et al. (2010) and Hülle (2011). After drying and sieving, all samples were treated with hydrochloric acid, sodium oxalate and hydrogen peroxide in order to remove carbonates, clay and organic material. As demonstrated by Hülle et al. (2010), the quartz fraction is not suitable for dating the sediments in the arid context in our study. They were contaminated with alkali-feldspars and that could not be eliminated by various techniques. Therefore, the feldspar fraction was chosen for dating. To separate the K-rich feldspar fraction for coarse-grain dating (100–200 μm), solutions of sodium polytungstate (2.68, 2.62, and 2.58 g cm^{-3}) were used.

The measurement parameters have been determined based on the SAR (single aliquot regenerative) protocols described by Murray

Table 1
Radiocarbon and luminescence results. * Two samples from the Orog Nuur are given as uncal. years BP.

Sample-No.	Field code/Lab.-No.	site	depth (cm)	coordi-nates (°)	dated material	OSL - age (ka)	^{14}C - age (cal yr BP)	OSL-fading corr. age (ka)
A: List of the sections of the Zavkhan Gol (ZG).								
ZG1_1	ME R-1	terr.	27	47.32 N - 95.83 E	dune sand	0.2 ± 0.1		0.3 ± 0.1
ZG1_2	ME R-3	terr.	120		dune sand	1.2 ± 0.1		1.4 ± 0.3
ZG1_3	ME R-4	terr.	140		dune sand	1.4 ± 0.1		1.7 ± 0.3
ZG2	C1/Erl-14424	dune	72	47.39 N - 95.87 E	charcoal		793 ± 63	
ZG3_1	Erl-14425		20	47.32 N - 95.77 E	charcoal		7268 ± 98	
ZG3_2	ME S-2	dune	100		dune sand	3.5 ± 0.3		4.0 ± 0.6
ZG4_1	Erl-14430		20	47.28 N - 95.95 E	charcoal		7268 ± 78	
ZG4_2	Buren, 5-1	dune	60		dune sand	11.2 ± 0.1		15.2 ± 1.4
ZG5_1	Erl-14426		20	47.45 N - 95.90 E	charcoal		7766 ± 60	
ZG5_2	Erl-14427		175		peat		9269 ± 113	
ZG5_3	CS 3a	terr.	250		dune sand	144 ± 13		144 ± 14
ZG5_4	CS 3b	terr.	280		dune sand	129 ± 11		129 ± 11
ZG5_5	CS 3c	terr.	400		dune sand	135 ± 11		135 ± 11
ZG6_1	ME-T1	lacustrine	30	47.32 N - 95.76 E	dune sand	119 ± 10		119 ± 10
ZG6_2	ME-T2	lacustrine	55		dune sand	127 ± 10		127 ± 10
ZG6_3	ME-T3	lacustrine	85		dune sand	114 ± 10		114 ± 10
ZG6_4	CS 1		205		dune sand	150 ± 13		150 ± 13
B: List of the sections of the Boon Tsagaan Nuur and Adagin Tsagaan Nuur (AT).								
AT1_1	HDS 044/15-38	lacustrine	150	45.58 N - 100.03 E	younger beach line	*1.4 ± 0.2*	*quartz dated,* Lehmkuhl and Lang (2001)	
AT1_2	HDS 045/15-39	lacustrine	190		younger beach line	*1.5 ± 0.2*		
AT2	HDS 046/16-40	lacustrine	100	45.58 N - 100.03 E	older beach line	*8.7 ± 1.0*		
C: List of the sections of the Orog Nuur (ON).								
ON1_1	ON-N1	dune	50	45.10 N - 100.82 E	dunesand	2.1 ± 0.2		2.6 ± 0.3
ON1_2	ON-N3	dune	135		dunesand	4.6 ± 0.4		5.2 ± 0.8
ON2_1	ON-NII-1	dune	40	45.12 N—100.81	dunesand	1.6 ± 0.1		1.8 ± 0.2
ON2_2	ON-NII-2	dune	100		dunesand	3.6 ± 0.3		4.3 ± 0.5
ON3	ON4	dune	100	45.04 N - 100.90 E	dunesand	0.7 ± 0.1		0.8 ± 0.1
ON4	SW2	lacustrine	60	45.04 N - 100.55 E	beach ridge	5.5 ± 0.5		6.7 ± 0.8
ON5_1	SW II 1	lacustrine	20	45.07 N - 100.61 E	beach ridge	2.8 ± 0.2		3.3 ± 0.4
ON5_2	SW II 2	lacustrine	70		beach ridge	3.5 ± 0.3		4.2 ± 0.5
ON6_1	HDS 047/17-41	lacustrine	100	45.18 N - 100.76 E	silt beach ridge	*79 ± 44*	*quartz dated* Lehmkuhl and Lang (2001)	
						75 ± 14	polymin. dated, Lehmkuhl and Lang (2001)	
ON6_2	HDS 049/17-44	lacustrine	300		silt beach ridge	*71 ± 11*	*polymin. dated,* Lehmkuhl and Lang (2001)	
ON Core II_1	ONW II/Erl-15628	lacustrine	1192	45.07 N, 100.58 E	core, bulk organic matter		*46,103 ± 2281**	
ON Core II_2	ONW II/Erl-15629	lacustrine	1272	45.07 N, 100.58 E	core, bulk organic matter		*40,429 ± 1340**	
D: List of the sections of the Taatsiin Tsagaan Nuur (TT).								
TT1_1	Erl-15408		5	45.14 N - 101.47 E	snail shells		3875 ± 109	
TT1_2	TAZ P1	playa	20		silty sand	2.9 ± 0.2		3.7 ± 0.2
TT1_3	TAP5/4	playa	120		silty sand	3.2 ± 0.2		4.0 ± 0.3
TT2_1	Erl-15316		4	45.12 N - 101.48 E	charcoal		4832 ± 137	
TT2_2	TAZ N1	Nugyn Els	15		dune sand	0.3 ± 0.1		0.4 ± 0.1
TT2_3	TAZ N3	Nugyn Els	60		dune sand	0.3 ± 0.1		0.4 ± 0.1
TT3_1	TAZ 1	lacustrine	170	45.20 N - 101.70 E	sandy beach ridge	120 ± 10		120 ± 10
TT3_2	TAZ 2	lacustrine	210		sandy beach ridge	108 ± 12		108 ± 12
TT4_1	TGT 1	T3 - terrace	500	45.30 N-101.15 E	dune sand	>400		>400
TT4_2	TGT 2	T3 - terrace	850		dune sand	>400		>400
E: List of the sections of the Ulaan Nuur (UN).								
UN1_1	Erl-15315		100	44.32 N - 103.6 E			4414 ± 153	
UN1_2	MoMä 2	T3 ? - terrace	160		fluv. sand	6.4 ± 0.5		7.8 ± 1.0
UN2_1	Mo 1	T3 - terrace	20	45.20 N - 104.1 E	fluv. sand	6.5 ± 0.7		8.1 ± 1.0
UN2_2	Mo 3	T3 - terrace	420		fluv. sand	11.1 ± 0.7		13.9 ± 1.4
UN3	Brig 3	T3 ? - terrace	100	44.65 N - 103.86 E	fluv. sand	162 ± 13		162 ± 13
F: List of the sections of the Bayan Tohomin Nuur (BT).								
BT1_1	BTF 1	u.alluv. fan	30	43.58 N - 103.20 E	fluv. sand	8.0 ± 0.8		12.6 ± 1.0
BT1_2	BTF 2	low. alluv.fan	100		fluv. silty-sand	15.7 ± 1.4		20.3 ± 2.7
BT2_1	BT1	dune	75	43.58 N - 103.20 E	dune sand	1.1 ± 0.1		1.4 ± 0.2
BT2_2	BT 2	dune	125		dune sand	1.5 ± 0.1		1.8 ± 0.2
BT2_3	BT 3	dune	170		dune sand	2.6 ± 0.2		3.3 ± 0.4
BT4_1	BT lake/Erl-13181	sedi. core	250	43.08 N –103.59 E	humic clay		6709 ± 45	
BT4_2	BT lake/Erl-12109	sedi. core	350		humic clay		9674 ± 85	
BT4_3	BT lake/Erl-13182	sedi. core	520		humic clay		6884 ± 64	
BT4_4	BT lake/Erl-12110	sedi. core	670		humic clay		12,661 ± 65	

Table 1 (*continued*)

Sample-No.	Field code/Lab.-No.	site	depth (cm)	coordi-nates (°)	dated material	OSL - age (ka)	14 C - age (cal yr BP)	OSL-fading corr. age (ka)
G: List of the sections of the Khongoryn Els and Ujim Sair (KE, US).								
KE1_1	US-Y	terr.	90	43.81 N–102.2 E	fluv. sand	4.3 ± 0.3		6.5 ± 0.5
KE2_1	US-Z		400	43.80 N–102.25 E	dune sand	15.2 ± 0.9		22.6 ± 1.6
KE3_1 (US)	US-A1	terr.	200	43.6 N - 102.35 E	dune sand	9.5 ± 0.9		11.9 ± 1.9
KE3_2 (US)	US-K	terr.	1500		dune sand	11.4 ± 0.7		14.3 ± 1.3
KE3_3 (US)	US-M	terr.	2000		dune sand	20.6 ± 1.2		27.1 ± 2.6
KE4 (US)	US-X	terr.	350	43.71 N–102.39 E	aeolian silt	8.6 ± 0.6		11.5 ± 1.2

Older quartz dated and polymineral dated samples from literature are given in italics.

and Wintle (2000) and Wallinga et al. (2000) for K-rich feldspar extracts. All luminescence measurements were carried out on automated Risø TL/OSL readers (TL-DA-15 or 20), which were equipped with 90Sr/90Y β-sources (dose rate of 0.11–0.15 Gy/s) for irradiation and with EMI 9235 photomultiplier tubes for luminescence detection. Based on the results of preheat tests, 270 °C for preheating of the regeneration dose as well as the test dose is appropriate to recover a given dose within 10% uncertainty. For each feldspar sample, 8 to 24 aliquots with 2 mm diameter were sufficient.

A signal loss called "anomalous fading" proved to be a problem in many dating studies using feldspars. As this may result in underestimation of the true burial dose, fading rates ("g-value") were determined following Auclair et al. (2003). To calculate fading corrected De values, the procedure proposed by Huntley and Lamothe (2001) was used (for some samples with neighboring g-values). For samples with ages >100 ka, fading-correction is complicated, as the natural signal is outside the linear part of the growth curve. Thomsen et al. (2008), Buylaert et al. (2009) and Thiel et al. (2011) showed that the post-IR IRSL signal using elevated stimulation temperatures has significant potential to derive a dating result that is far more independent from fading-correction than the conventional $IRSL_{50°C}$-signal. Therefore, the protocol suggested by Thiel et al. (2011) was selected for "old" samples (>ca.50 ka), using a stimulation temperature of 290 °C after preheating at 320 °C and an IR bleach at 50 °C. The general quality criteria indicate applicability of the protocol.

To calculate a burial age of a sample, the environmental dose-rate has to be determined, which is created by the radioactive elements existing in grains of the sample and surrounding sediment, with a contribution from cosmic rays. For the samples analyzed in this study, laboratory high resolution gamma-spectrometry was conducted to obtain the contribution from uranium (U) and thorium (Th) decay chains and from potassium (K). All measurements were converted to alpha, beta and gamma dose rates according to the conversion factors of Aitken (1998). For K-feldspars an internal potassium content of 12.5 ± 0.5% (Huntley and Baril, 1997) and an α-efficiency factor of 0.07 ± 0.02 (Preusser et al., 2008) was assumed. The dose rate from cosmic rays was calculated on the basis of sample burial depth and the altitude of the section (Prescott and Hutton, 1994). The dose rate was calculated taking variations in the water content of 0–20 weight-%, depending on the actual water content and the porosity, into account.

For comparison, 5 older luminescence data (3 sections) from Lehmkuhl and Lang (2001) are in Table 1B and C. As these have been determined on quartz samples, they have to be regarded with reservations.

3.2.2. *Radiocarbon dating*

Radiocarbon dating (see Table 2) was carried out on 12 samples from in situ peat within sandy and gravelly fluvial sediments as well as charcoal and mollusk shells. The datings were carried out in the AMS – lab. of Erlangen University. All data were calibrated with CalPal-online and the CalPal2007-HULU curve (Weninger et al., 2007). In the following, most radiocarbon ages are presented as calibrated years (cal. BP). However, many samples for radiocarbon dating in central Asia are affected by the so-called reservoir effect. This effect describes the incorporation of older carbon in an organism (Lockot et al., 2016). The actual hard-water effect can be determined by the evaluation of the radiocarbon age of a living species and can reach values of up to 20 ka (Mischke et al., 2013). However, in many samples it is much lower and ranges between several hundred to 3000 years. Nevertheless, the hard water effect varies trough time (Long et al., 2011). For this study, it was not determined as mainly individual samples were taken. Therefore, all the radiocarbon ages have to be regarded as minimum ages.

4. Results and data interpretation

4.1. *Valley of the Great Lakes*

4.1.1. *Zavkhan Gol*

The floodplain of the Zavkhan Gol shows a pattern of numerous meanders, indicating a swampy area with modern periodical inundations (Fig. 2, Fig. S1). The plain is dried out nowadays, as observed during fieldwork in 2007 and 2008. Nevertheless, at numerous places, patches of light-grey silt occur as evidence of a marked environmental change since 1960. Revealed by fieldwork along the middle reach of the Zavkhan Gol, the desiccation is not primarily due to a climate change but to human influences. Near the settlement of Guilin (46.4°N, 96.7°E), an irrigation project was built in the late 1960 years consuming about 50% of the freshwater. Today the project is closed but the irrigation channel is still in full function and the water loss of the Zavkhan Gol is continuing (Hülle, 2011; Stolz et al., 2012).

The reconstruction of paleolakes on the Zavkhan Gol floodplain, based on a couple of dates from the eastern rim of Mongol Els (see Stolz et al., 2012), may serve as a base to understand and to classify such phenomena in the Valley of Gobi Lakes more to the south (see 4.2). Therefore, it is of high interest to create a synopsis including all basins presented here.

4.1.1.1. Mid-Pleistocene sediments. Near the 130 m high eastern front of the Mongol Els dune field and within dune valleys inactive humble dunes locally with lots of mollusc shells on top occur. On top of such a dune, located approx. 17 m above the floodplain, the following section was found (ZG 6 in Fig. 2, 1437 m a.s.l., 47.31°N, 95.74°E; ME 5A in Hülle, 2011; Stolz et al., 2012): The top (0–15 cm) is formed by strongly disturbed, carbonate silt with numerous mollusc shells pointing to lacustrine deposition. Between 15 and 80 cm depth, thick silt layers are interbedded by thin dune sand layers, both disturbed due to former frost activity. The latter ones

Table 2
Radiocarbon dating results. The ZG-samples are adapted from Stolz et al. (2012), the BT-samples from Felauer et al. (2012).

Sample-No.	Lab.-No	Depth (cm)	^{14}C age and error (yr BP)	Delta ^{13}C	Calibrated age (cal. yr BP)	Material
ZG2	Erl-14424	72	853 ± 42		793 ± 63	charcoal
ZG3_1	Erl-14425	20	6332 ± 88	−4.6	7268 ± 98	carbonatic silt
ZG4_1	Erl-14430	20	6328 ± 68	−4.5	7268 ± 78	carbonate
ZG5_1	Erl-14426	20	6923 ± 57	−24.8	7766 ± 60	humic sediments
ZG5_2	Erl-14427	190	8274 ± 65	−25.4	9269 ± 113	peat
ON Core II_1	Erl-15628	1192	46,103 ± 2281	−25.4	45,687 ± 2364	bulk sample
ON Core II_2	Erl-15629	1272	40,429 ± 1340	−24.9	42,216 ± 2123	bulk sample
TT1_1	Erl-15408	5	3577 ± 77	−14.3	3875 ± 109	gastropode shells
TT2_1	Erl-15316	4	4279 ± 86	−22.9	4832 ± 137	charcoal
UN1_1	Erl-15315	100	3956 ± 102	−25.1	4414 ± 153	bulk sample
BT4_1	Erl-13181	253	5880 ± 46	−20.5	6709 ± 45	bulk sample
BT4_2	Erl-12109	353	8697 ± 56	−22.7	9674 ± 85	bulk sample
BT4_3	Erl-13182	526	6037 ± 47	−21.6	6884 ± 64	bulk sample
BT4_4	Erl-12110	674	10,661 ± 56	−23.3	12,661 ± 65	bulk sample

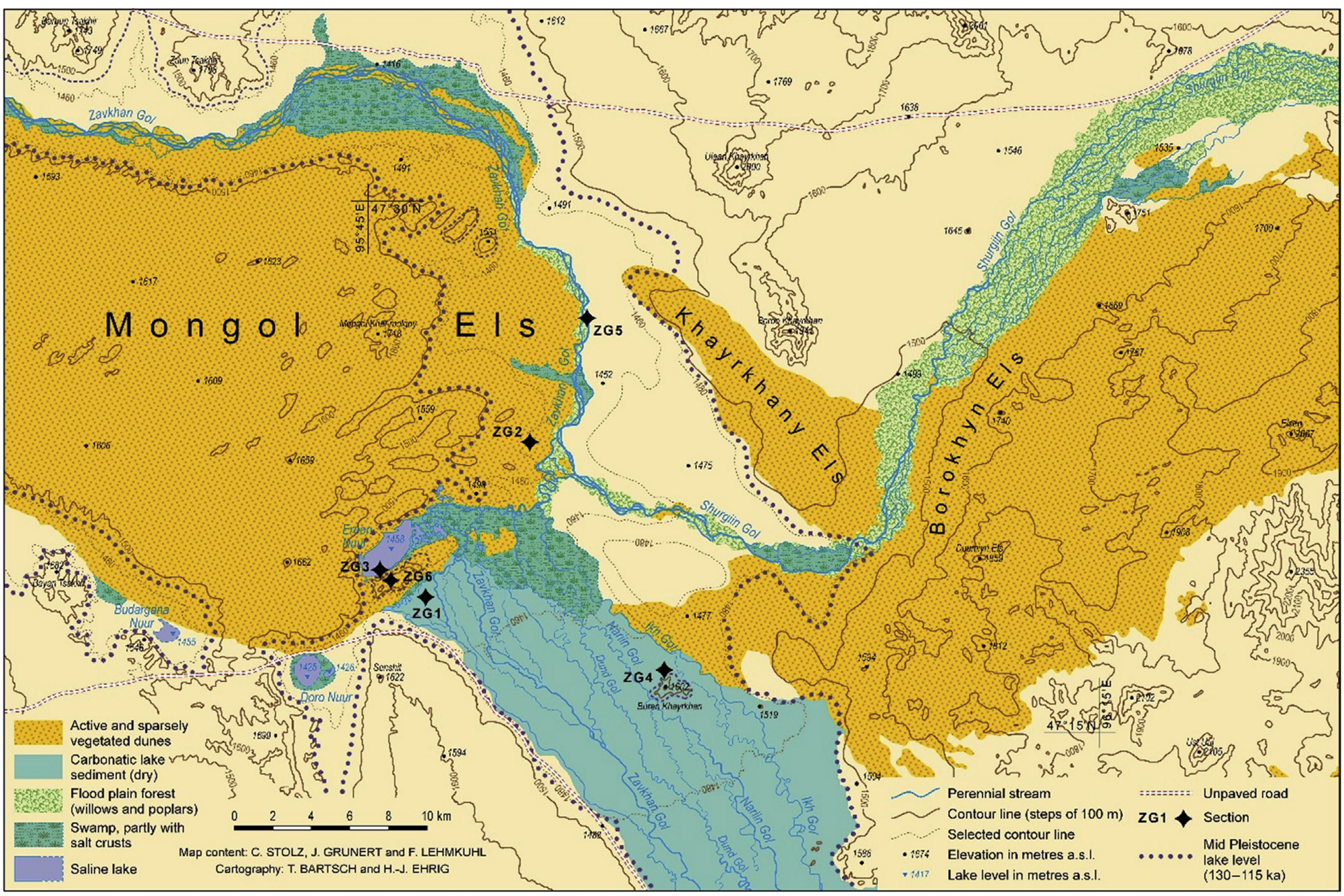

Fig. 2. Map of the floodplain of Zavkhan Gol and Mongol Els. Modified from Stolz et al. (2012).

become more dominant downward until 190 cm depth. Pure dune sand was found below 190 cm depth. Dune sand layers within the likely lacustrine sediment body were OSL–dated at depths of 30 cm, 55 cm and 85 cm to 119 ± 10 ka (ZG6_1), 127 ± 10 ka (ZG6_2), and 114 ± 10 ka (ZG6_3), respectively. Pure dune sand at 205 cm depth was OSL-dated to 150 ± 13 ka (ZG6_4) placing the formation of dune sand into MIS 6. The lacustrine sediment above (carbonate content 15%) indicates an Eemian age (MIS 5e) and allows reconstructing a giant lake of nearly 600 km^2 and 17 m depth. However, the lake did not exist during MIS 6.

The OSL age of the dune sand at 205 cm depth (150 ± 13 ka) can be well compared with the three ages of the cut-off slope of the Zavkhan Gol (ZG 5 in Figs. 2 and 3, 1455 m a.s.l., 47.4°N, 95.9°E). Section ZG 5 (Stolz et al., 2012) shows a silty sediment on top underlain by fluvial gravel and peat layers and from 190 cm to 410 cm depth dune sand interbedded with thin gravel layers. Both sediments are clearly separated by an unconformity. The deepest part of the profile near the river bed at 500 cm depth is represented by fluvial gravel. OSL-dating of dune sand at depths of 250 cm, 280 cm, and 400 cm provide ages of 144 ± 13 ka (ZG 5_3), 129 ± 11 ka (ZG 5_4), and 135 ± 11 ka (ZG 5_5), respectively. A periodical damming effect by dune sands of a postulated Eemian paleolake can be

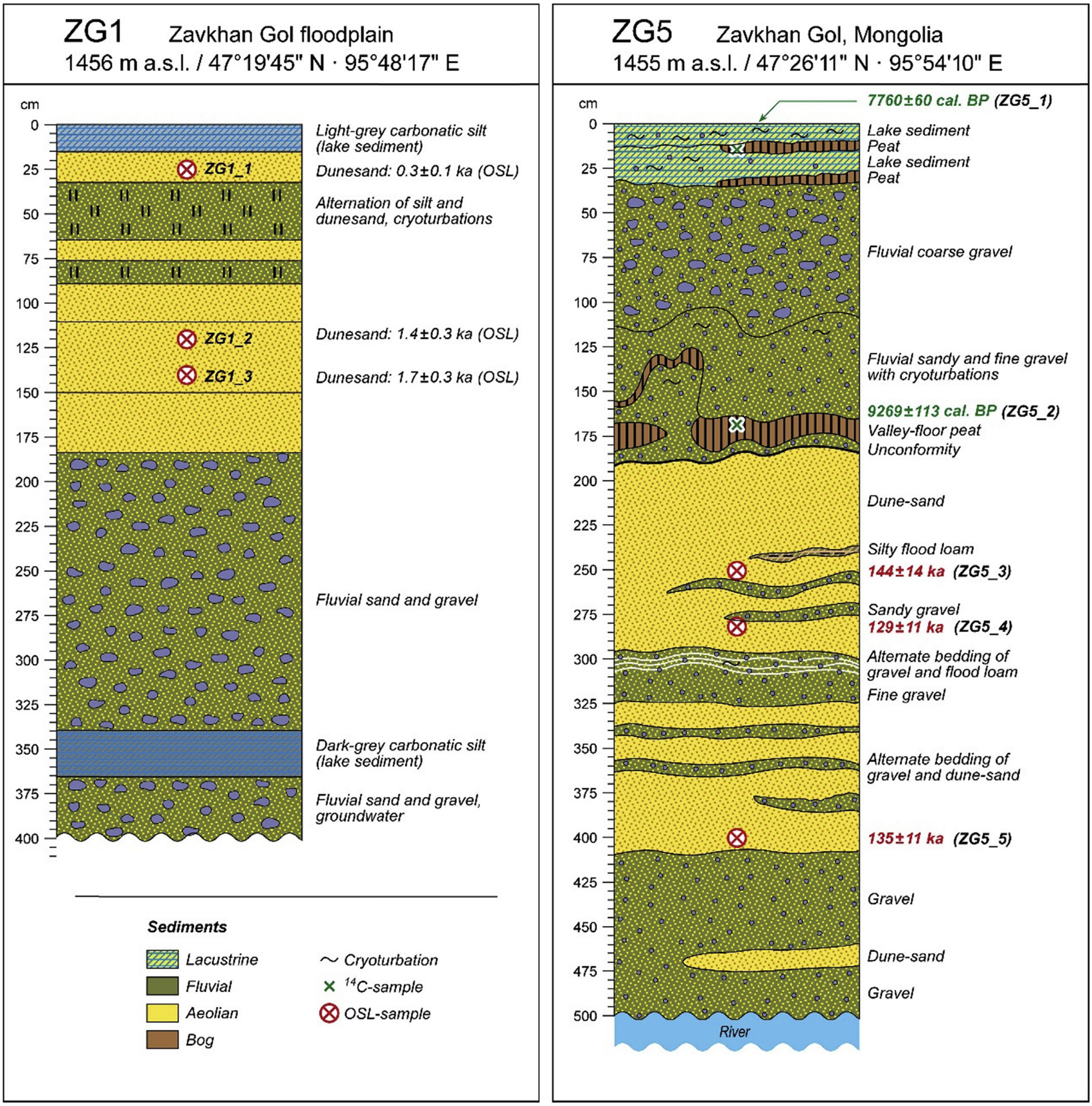

Fig. 3. Sections ZG1 and ZG5 in the vicinity of the Zavkhan Gol. Modified from Stolz et al. (2012).

derived from their alternation with gravel layers. The area is regarded as an interaction zone of eolian and fluvial processes in the late Quaternary.

4.1.1.2. Sediments of the Late Glacial to the early Holocene. Lacustrine silty sediments on top of the 5 m high cut-off slope of the Zavkhan Gol (see above, ZG 5 in Figs. 2 and 3; 1455 m a.s.l., 47.3°N, 95.75°E, C2 in Stolz et al., 2012) are strongly cryoturbated. Charcoal found near the top was dated to 7766 ± 60 cal. BP (ZG5_1). Below the silty sediment fluvial gravel reached at depth of 190 cm. At the bottom of these gravels a peat layer was radiocarbon dated to the early Holocene (9269 ± 113 cal. BP, ZG5_2).

The silty, carbonate-rich sediment, which was found in a dune valley 1 km west of the dune front and 5 m higher than the level of the floodplain (ZG3 in Fig. 2, 47.31°N, 95.74°E), was dated by radiocarbon AMS to 7268 ± 98 cal. BP (ZG3_1). The dune sand below was dated by OSL to 4.0 ± 0.6 ka (ZG3_2), which indicates a mid-Holocene deposition time and a likely high reservoir error for the radiocarbon age if the OSL age is correct. However, in comparison with the ages from nearby sections (see below) the OSL age seems to underestimate the age of deposition by more than 3 ka.

The isolated mountain Buren Khayrkhan in the center of the

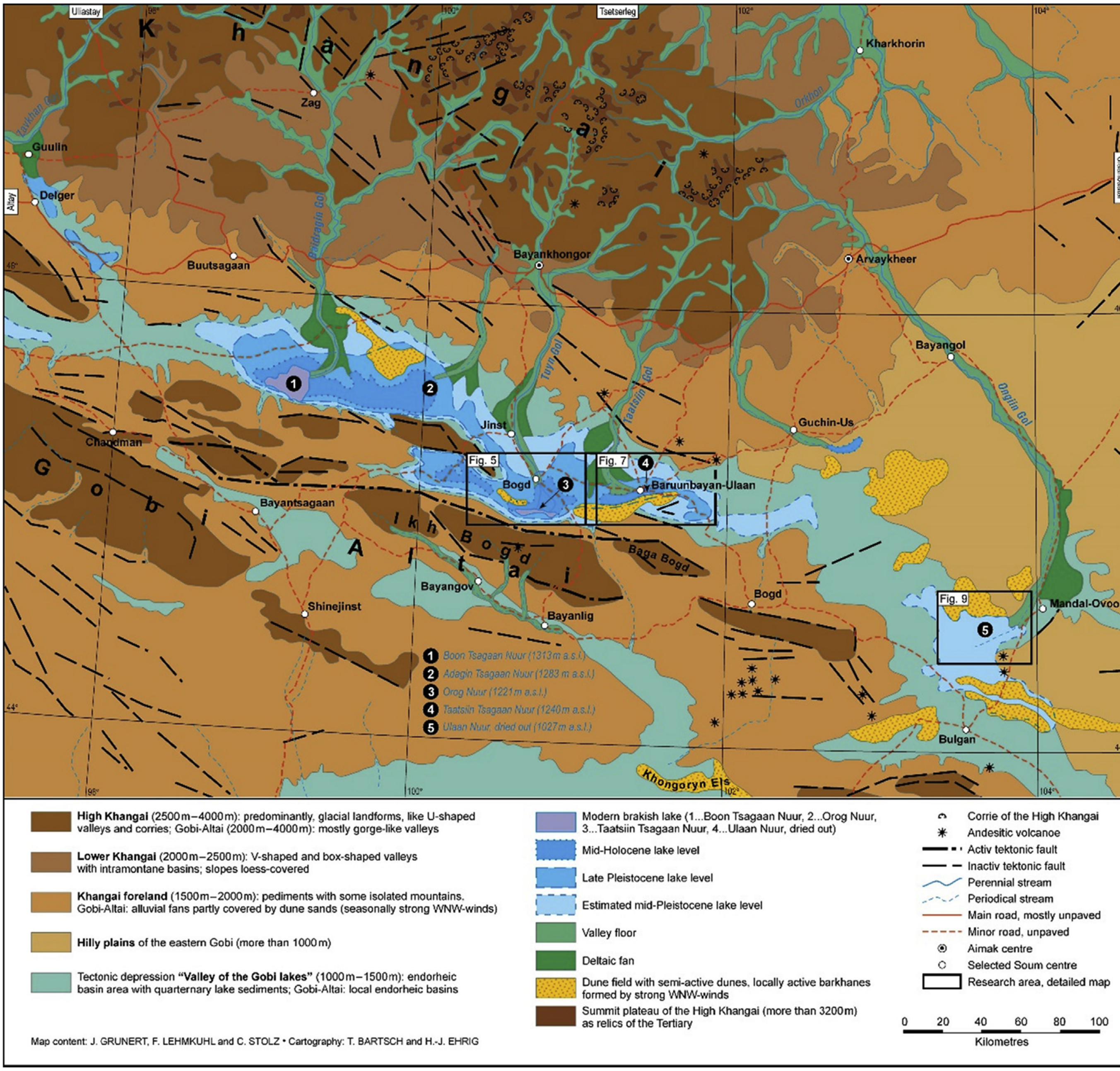

Fig. 4. Geomorphological map of the "Valley of the Gobi Lakes" and adjacent areas based on Deviatkin et al. (1987) and the topographical maps of Mongolia 1:500.000.

floodplain of the Zavkhan Gol (1.464 m a.s.l.) is surrounded by humble dunes in a shallow depression on its western and northern foreland, in which silty (lake) sediments were found (ZG4 in Fig. 2, 47.30°N, 96.0°E). Incorporated charcoal was radiocarbon dated to 7268 ± 78 cal. BP (ZG4_1). The sand below was OSL-dated to 15.2 ± 1.4 ka (ZG4_2; Stolz et al., 2012).

The sediments of these three locations allow the reconstruction of an early Holocene shallow lake between 7200 and 9200 cal. BP with a depth of 6–7 m and an area of nearly 50 km^2.

4.1.1.3. Sediments of the late Holocene. Exposure ZG1 (47.32°N, 95.83°E) is located 300 m east of the dune front at a cut-off slope of a dried-out oxbow-lake of the Zavkhan Gol (Fig. 3) (Stolz et al., 2012). The top is represented by clayey floodplain deposits likely deposited in shallow ponds. The sediments at 25 cm depth were dated to 0.3 ± 0.1 ka (ZG1_1). The middle part of the section, up to 185 cm depth, consists of alternations of dune sand and floodplain deposits. The lower part of the section revealed by drilling consists of fluvial sand and gravel interrupted at 340–365 cm depth by a silt deposited in a shallow lake. Dune sands in 120 and 140 cm depth provided an ages of 1.4 ± 0.3 ka and 1.7 ± 0.3 ka (ZG1_2, ZG1_3). At a nearby position but 250 m west of the dune front within a dune depression a silty, carbonate-rich sediment 0.5 m above the level of the floodplain was found (see ZG2 in Fig. 2; C 1 in Stolz et al., 2012). Charcoal in 72 cm depth was radiocarbon dated to 793 ± 63 cal. BP (Erl. 14424). We interpret the silty sediments as remnants of a shallow pond along a former Zavkhan Gol meander. Since the desiccation of the pond, the dune front moved eastward for about 250 m.

Summarizing the texture of lacustrine silt sediments at four different sites on or close to the level of the floodplain (ZG1, ZG2, ZG3 and ZG4) similar contents of silt (about 40%) and, together with clay and very fine sand, contents of more than 60% were measured (see supplement Tables S1 and S2 for the grain size of ZG1 and ZG5). The carbonate contents of 8–10% are comparable too, except ZG5 with 16%. The texture of lacustrine silts at higher positions above the level of the floodplain (ZG3: 5 m and ZG6: 17 m) is similar too. The carbonate content in ZG3 was measured to 8%; in the top layer of ZG6 to 15%. Only at this place numerous mollusc shells were found.

Regarding the dune sand layers of all six sections a resembling of the textures is obvious too. Fine and medium sands are dominant (together more than 80%); coarse sands and gravels are lacking. The carbonate contents are very low.

4.2. Valley of Gobi Lakes

In the following we describe five main basins in the Valley of Gobi Lakes (Boon Tsagaan Nuur and Adagin Tsagaan Nuur, Orog Nuur, Taatsiin Tsagaan Nuur, Ulaan Nuur) in detail. Fig. 4 provides an overview including lake level variations during the late Quaternary.

4.2.1. Boon Tsagaan Nuur and Adagin Tsagaan Nuur

Boon Tsagaan Nuur (No. 1 in Fig. 4; 1300 m a.s.l.) is a 30 × 20 km large brackish lake and represents the only perennial one in the Valley of the Gobi Lakes. The dried out basin of Adagin Tsagaan Nuur is located about 60 km east (No. 2 in Fig. 4; 1283 m a.s.l.). Both are terminal lakes of the Baidragin Gol. The latter drains the central Khangai. All higher peaks and mountains (up to 3,500 m a.s.l.) were glaciated during the last glacial maximum (Lehmkuhl, 1998; Walther, 1998; Lehmkuhl and Lang, 2001) resulting in a decrease in the equilibrium line altitude (ELA) of around 1000 m from about 3800 m a.s.l. to 2800 m a.s.l.

The existence of larger paleolakes is indicated by a series of three beach ridges in both basins (Komatsu et al., 2001). The beach ridges are at 1326, 1331 and 1370 m a.s.l. at the Adagin Tsagaan Nuur (Lehmkuhl and Lang, 2001). The modern lake level is at 1300 m a.s.l. As the watershed between the Boon Tsagaan Nuur and the Adagin Tsagaan Nuur is below 1330 m a.s.l., the two higher beach ridges indicate a large paleolake covering both basins. The paleolake related to the beach ridge at 1331 m a.s.l. had a length of some 150 km and covered an area of about 1920 km^2, based on area calculations using remote sensing data. This is further supported by a cliff at the southern margin Boon Tsagaan Nuur at a similar elevation (Lehmkuhl and Lang, 2001). During the formation of the highest beach ridge a giant paleolake formed which drained into the basin of the Orog Nuur.

The sediments of the lowermost beach line at 1326 m a.s.l. date to 1.4 ± 0.2 (AT1_1) and to 1.5 ka ± 0.2 (AT1_2) while the lakeshore at 1331 m a.s.l. was OSL dated to 8.7 ± 1.0 ka (AT2) (Lehmkuhl and Lang, 2001; Figs. S2 and S3). During the late Holocene two individual lakes existed in the basins of the Boon Tsagaan Nuur and the Adagin Tsagaan Nuur, while during the early Holocene a large lake covered both basins.

4.2.2. Orog Nuur and Taatsiin Tsagaan Nuur

The basins of the Orog Nuur (1221 m a.s.l; No. 3 in Fig. 4, Fig. S5) and the Taatsiin Tsagaan Nuur (1240 m a.s.l., No. 4 in Fig. 4, Fig. S13) are bordered by the wide foreland of the Khangai in the north and to the south by the high mountain ranges of Ikh Bogd (3900 m a.s.l.) and Baga Bogd (2400 m a.s.l.), both belonging to the Gobi Altai Mountains. In the 1: 100,000 (published in 1960) and 1:500,000 topographic map of Mongolia (Geodesy and Cartography Agency of Mongolia, 1978), the lake levels of Orog Nuur and Taatsiin Tsagaan Nuur are marked at 1221 m and 1241 m a.s.l., respectively. Shallow but permanent lakes existed at that time. Today they were only filled during summers when the rainfall is above average. This was the case in August 2007 when the discharge of the Tuyn Gol, which nourishes the Orog Nuur, was remarkably high. In August 2008, when the discharge was low, the lake bottom remained dry.

4.2.2.1. Orog Nuur. Paleolake-levels of the Orog Nuur occur at 3 m, 10 m, 16 m (lake level 1 = L.L.1 in Fig. 5) and 23 m (L.L.2) above the lake level adapted from the topographical map. In the last decades the lake level fluctuated and in some year's large part of the lake dried out (Szumińska, 2016; Walther et al., 2016). The higher lake levels were described by Walther (1998), Lehmkuhl and Lang (2001), Hülle (2011), and Walther et al. (2016). An additional lake shore was recognized 60 m above the present lake level (L.L.3) (Lehmkuhl and Lang, 2001). Carbonate–rich silty lake sediments occur at several places within the dune-covered area north of the lake. Fig. 5 provides an overview of the different lake levels in the Orog Nuur basin.

Fig. 6 provides a sketch of the different lake levels north of the Orog Nuur. A silty sediment two km north of the lake basin and 9 m above the lake bottom within a coppice dune field was dated by OSL to 5.2 ± 0.8 ka (135 cm depths ON1_2) and 2.6 ± 0.3 ka (50 cm depths ON1_1), indicating a mid-to-late Holocene age for this supposed lake level (see also Table S4). Another silty sediment three km north of ON1, 15 m above the lake bottom, but also within the coppice dune field, was dated by OSL to 4.3 ± 0.5 ka (section ON2; 100 cm depths ON2_2; Table S5) and 1.8 ± 0.2ka (40 cm depths ON2_1). Further silty lake sediments near the 16 m level were found within the dune field bordering the lake basin in the east (ON3). One OSL-date provides a young age of 0.8 ± 0.1 ka (100 cm depths ON3; see Table 1C) which is an indication of the last aeolian period due to dune sand remobilization. The OSL ages from L.L. 1 indicate higher than-present lake levels during the mid-to late Holocene.

The 23 m level (L.L. 2 in Figs. 5 and 6 and Fig. S7 – S10) is marked by a conspicuous gravelly embankment interpreted as beach ridge in the area surrounding the western lake basin. ON4 (45.104° N, 100.55° E) is located in a channel incised in the beach ridge (Hülle, 2011). The sand in 60 cm depth was OSL–dated to 6.7 ± 0.8 ka. Section ON5 (45.07°N, 100.61°E; Table S7) is a profile dug on the gravel-rich beach ridge at the northwestern rim of the basin. Sand layers at depths of 70 cm and 20 cm were OSL-dated to 4.2 ± 0.5 ka (ON5_2) and 3.3 ± 0.4 ka (ON5_1), respectively. It was not possible to reach the base of the coarse gravels. In summary, the OSL-dates of ON4 and ON5 and of ON1 and ON2, are pointing to deposition during mid-Holocene time. A large lake occupied the basin at that time. It was likely nourished predominantly by the Tuyn Gol. Compared with the results described above (see 4.1.1 and 4.2.1) it seems reasonable to infer similar lake development here.

12 km north of Orog Nuur and 3 km west of the small settlement of Bogd, the following sequence was found in 1280 m a.s.l. (ON6 and L.L. 3 in Fig. 5). Remnants of bedded and unbedded lacustrine sediments, covered by gravel of younger alluvial phases (see Figs. S11 and S12 and Table S8). The gravels were previously correlated with the Last Glacial period, when all the alluvial fans were active (see Grunert et al., 2000; Lehmkuhl and Lang, 2001). The size of this lake was approximately 1040 km^2, ten times larger than that of present day (map of 1960). However, this huge paleolake might have had a larger extent towards the east including the Taatsiin Tsagaan Nuur basin (see Fig. 4). These sediments of the highest beach line of the Orog Nuur (section ON6) provide luminescence ages of about 70–80 ka (Table 1C; ON6_1, ON6_2: Lehmkuhl and Lang, 2001) and provide evidence for very high lake levels at the beginning of the Last Glacial period (more details are

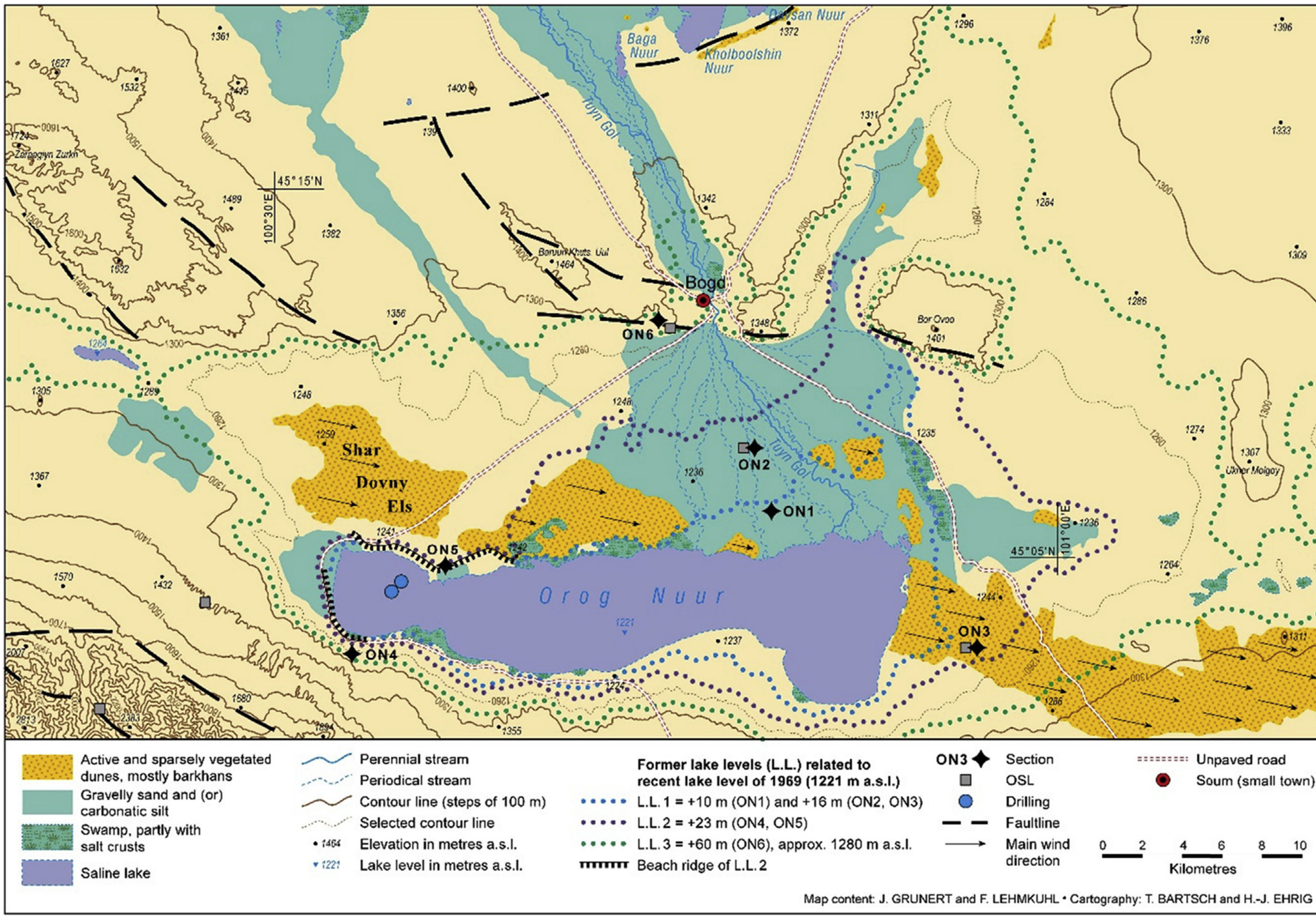

Fig. 5. Geomorphological map of the Orog Nuur depression.

given in the supplement).

Two parallel cores (ONCore II_1, 6.00 m; ONCore II_2, 13.35 m) were retrieved from Lake Orog Nuur (Felauer, 2011; Yu et al., 2016, 2017). The radiocarbon and pollen data show a marked moisture pulse during the Marine Isotope Stage 3 which might have induced the maximum last glacial expansion in the high elevated Khangai Mountains (Rother et al., 2014; Lehmkuhl et al., 2016).

4.2.2.2. Taatsiin Tsagaan Nuur. The Taatsiin Tsagaan Nuur is situated east of the Orog Nuur (see Fig. 4, No. 4 and Fig. 7; Fig. S13). Today, the lake is dried up and the lake bottom is covered by white, slightly salty silt. The Taatsiin Gol also originated in the Khangai Mountains but is much smaller than Tuyn Gol. Fig. 7 provides a map of the basin with different lake levels (L.L.), dunes and locations of the sections. The northern rim of the lake is formed by a gravelly beach ridge of 8 m height, which is similar to the 23 m-beach ridge of Orog Nuur (L.L. 2).

Section TT1 (45.20° N, 101.25° E, Figs. 7 and 8, Table S9) was dug into a playa-like sediment at the southern rim of Taatsiin Tsagaan Nuur. OSL ages of 5.0 ± 0.3 ka at 120 cm (TT1_3) and 3.9 ± 0.2 ka at 20 cm depth (TT1_2) suggest mid Holocene ages. Gastropod shells at a depth of 5 cm were ^{14}C–dated to 3875 ± 109 cal. BP (TT1_1, Erl-15408), and correspond to the OSL data.

Section TT2 (45.12° N, 101.48°E, Fig. 8, Figs. S14–S16, Table S10) was located 1 km to the south within the dune area of Nugiin Els. Remnants of silty carbonate lake sediments 8 m above the lake bottom were found here. They were OSL-dated to 0.4 ± 0.1 ka at 60 cm (TT2_3) and 0.4 ± 0.1 ka at 15 cm depth (TT2_2). Both dates are much younger than the radiocarbon ages of charcoal enclosed in the silt, which was dated to 4832 ± 137 cal. BP (TT2_1, Erl. 15316). The reason for this discrepancy remains unknown.

The 7 m high gravelly terrace 15 km east of the Taatsiin Tsagaan Nuur (section TT3 in Fig. 7, 45.20°N, 101.70°E, 1280 m a.s.l., Fig. S17 – S20, Table S11) is completely different. It likely represents the remnant of a very old beach ridge 40–43 m above the lake bottom named L.L. 3. We assume that a giant paleolake was connected with the paleolake of Orog Nuur represented by its 60 m-level (see above). Sand layers in 210 cm and 170 cm depths were OSL-dated to 108 ± 12 ka (TT3_2) and 120 ± 10 ka (TT3_1), respectively. The ages from the Orog Nuur were 70–80 ka, and therefore 30 to 40 ka younger. A larger paleolake might have existed in the area during the last interglacial (MIS 5e) until the early last glacial. However, the number of ages is still relatively small. A 40 m beach ridge (L.L.3) 10 km west of Taatsiin Tsagaan Nuur (see Fig. S13) was not investigated during field work.

4.3. Ulaan Nuur and Ongiin Gol

4.3.1. Ulaan Nuur

The most eastern depression in the Valley of the Gobi Lakes is covered by the Ulaan Nuur (1027 m a.s.l.; No. 5 in Figs. 4 and 9, Fig. S21). This basin has an isolated position compared with the other ones. It represents the terminal depression of the Ongiin Gol which drains the high eastern Khangai. The summits in the

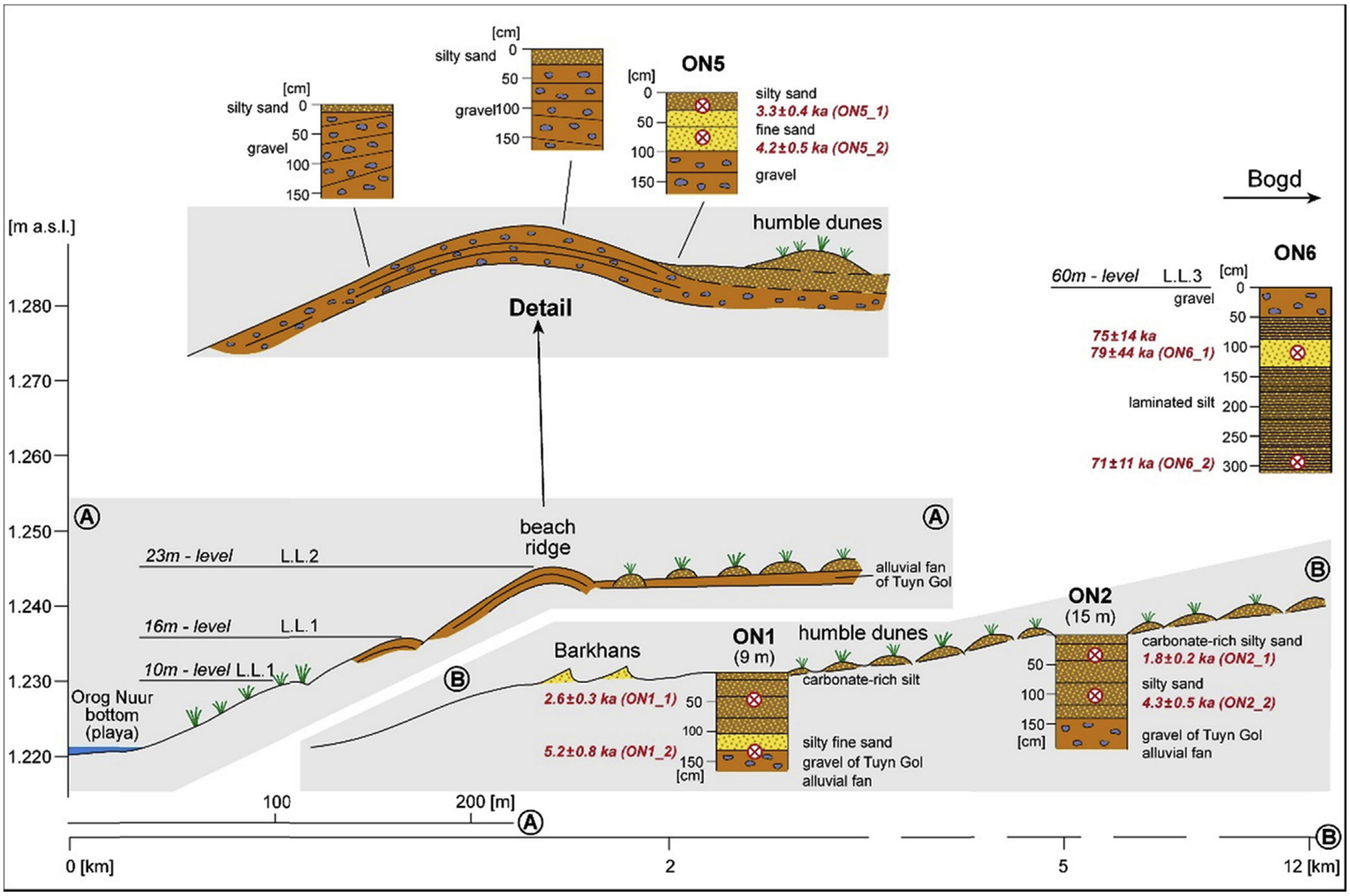

Fig. 6. South – North cross section north of the Orog Nuur indicating the different lake levels.

catchment were glaciated during the LGM (Lehmkuhl, 1998; Rother et al., 2014). A large amount of water from the Ongiin Gol is currently used for settlement purposes along the mountain rim especially for the freshwater supply of the city of Arbaykheer. A photograph from 1920 (stored in a monastery) showed a high discharge of in the middle reach the river. As reported by a monk, high discharge during the summer was common until the 1960s. Until this time, the Ulaan Nuur was a permanent lake. Nowadays the lake is dried out and the former lake bottom is partly covered by barkhan dunes. The most recent lake level highstand until the 1960s was 2–3 m above the present dry lake bottom. An older beach ridge 13 m above the lake bottom was found at the eastern rim of the basin (L.L. 2 in Figs. 9 and 10; UN1 in Fig. S22).

Section UN1 (Fig. 10, Figs. S22 and S23; Table S12) was located at a cut-off slope of the Ongiin Gol a few km upstream of the lake basin (L.L. 2: 1040 m a.s.l., 44.32 N, 103.6 E). Here a smoothened beach ridge was detected. A humic layer at 100 cm depth was ^{14}C–dated to 4414 ± 153 cal. BP (UN1_1, Erl. 15315). A layer of fine sand at 160 cm depths was OSL-dated to 7.8 ± 1.0 ka (UN1_2). Both dates are of mid-Holocene age. At that time, a lake of approximately 500 km^2 in size could have existed, albeit to reconstruct its shape remains speculative due to missing well expressed shore lines at the lake (see Fig. S21).

4.3.2. Ongiin Gol

Indications for a Late Glacial to early Holocene fluvial activity were found at a 6 m high cut-off slope of the main terrace (T3) of the river some 55 km NNE of Ulaan Nuur (UN2: 1195 m a.s.l., 45.05°N, 104.6°E). The sediment structure of the profile UN2 is shown in Fig. 10, Fig. S24 and Table S13.

At the surface up to a depth of 30 cm, compacted grey silty sand was observed. Underneath to 370 cm depth, well bedded silty to sandy gravel with fanglomerate were found. Fine sand in all probability of eolian origin between 370 and 430 cm depth was followed by grey granite grus and gravel up to a depth of 600 cm. These successions are typical for the LGM as observed at several terrace sites along all large rivers in the southern Khangai foreland. The summits of the Khangai above 3000 m were glaciated during the LGM and provide a lot of gravel.

A lens of fine sand at 20 cm depth was OSL-dated to 8.1 ± 1.0 ka (UN2_1) ranging the silt on top into early Holocene. The eolian fine sand at 420 cm depths was OSL-dated to 13.9 ± 1.4 ka (UN2_2) indicating deposition already during the Late Glacial period.

In the lower reaches of the Ongiin Gol, the drainage valley transforms into a broad floodplain, which is bordered to the east by the 10 m high slope of an extended terrace. It represents the main terrace (T3) of Ongiin Gol. Section UN3 (45.05°N, 104.05°E, Fig. 9; Fig. S25) was situated in a gully at the terrace-slope some 20 km upstream of section UN1. Sedimentological data are given in Table S14. The surface sediments consisted of a 10 cm thick dark brown gravel layer, followed by white carbonatic silt down to 50 cm depth, strongly deformed by cryogenic processes. Such cryoturbations also affected the following gravels down to 200 cm depth. A sand layer at 100 cm was OSL-dated to 162 ± 13 ka (see Table 1E). The silty sediments are interpreted as lake sediments. During that period, a giant paleolake of ~43 m depths might have existed. It may be compared with the old paleolakes described for the other lake basins, albeit its shape remains still speculative. In

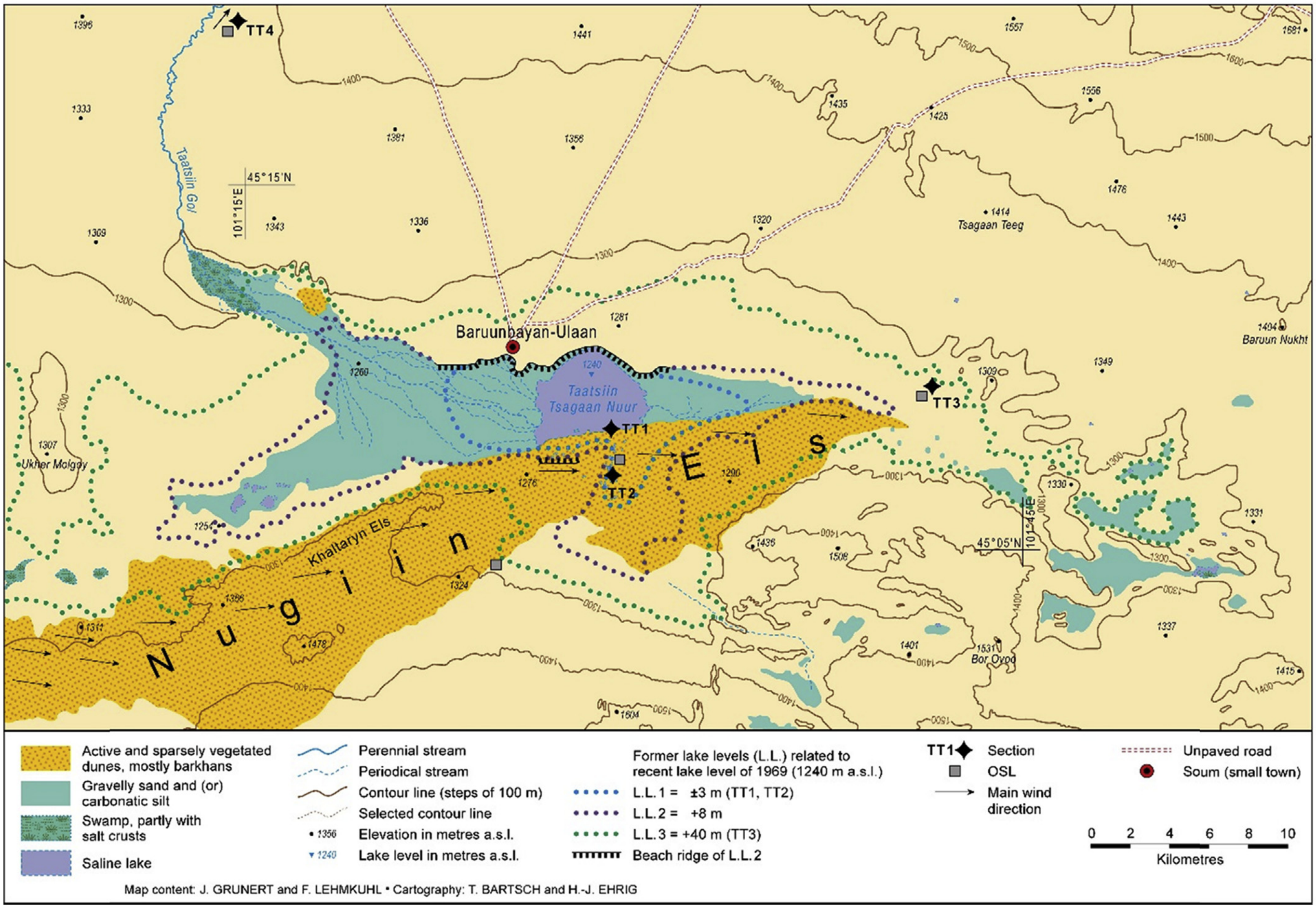

Fig. 7. Map of the Taatsiin Tsagaan Nuur.

accordance with the age of the sand layer below, the paleolake formed after the MIS 6.

4.4. *Bayan Tohomin Nuur and Khongoryn Nuur*

Compared with the lake basins in the Valley of the Gobi Lakes, the basins to be described now are smaller in size and located further south. They belong to a tectonic depression running WNW – ESE some 170 km south of the Valley of the Gobi Lakes and are bordered on both sides by local ranges some 2500 m height (Figs. 1 and 11, Baljinaym et al., 1993). The annual mean precipitation is estimated to be less than 100 mm in the basins and 150–200 mm in the summit areas (Academy of Sciences of Mongolia and Academia of Sciences of USSR, 1990).

4.4.1. *Bayan Tohomin Nuur*

The basin of the Bayan Tohomin Nuur (1417 m a.s.l.) was investigated in 2007 and 2008 (Grunert et al., 2009; Felauer, 2011; Felauer et al., 2012). It is merely 30 km^2 wide and today completely dried out. To the west and south it is bordered by the Khongoryn Els dune field, the dunes of which are only 10 m high and partly fixed by *Nitraria*. To the north there is a 6–7 km wide pediment composed of alluvial fans in the foreland of a 2500 m high range (Fig. 11). At a 120 cm high cut-off slope of a fan-channel 1.5 km north of the old shoreline of a paleolake (43.58°N, 103.20°E), the following sediment-sequence was exposed (BT1; Fig. S26): Between the surface and a depth of 50 cm, non-compacted fanglomerates are interbedded with sand layers. Up to depth of 120 cm, there are compacted fanglomerates interbedded with sand and silt layers. Both layers are separated by an unconformity. Sand at 30 cm and 100 cm depths was OSL-dated to 12.6 ± 1.0 ka (BT1_1) and 20.3 ± 2.7 ka (BT1_2), respectively. The sand layers are of fluvial origin. Combined with the fanglomerates they indicate a slightly higher humidity in the catchment of the Bayan Tohomin Nuur.

The shoreline of the some 30 km^2 wide paleolake is marked by a ridge of small dunes covered by dense grass vegetation. A profile (BT2, Fig. 12 and Figs. S27 and 43.58°N, 103.20°E) dug at the seaward side of a dune presents the following sediment sequence:

The first 170 cm of the section consists of well-bedded silty and dry dune sand. Underneath between 170 and 200 cm depth, small-sized, water-saturated fanglomerates were found (1427.0 m a.s.l.). This layer is interpreted as the upper layer of the fan which stretches towards the basin. An extended thufur spring bog developed on its gentle slope. Deeper layers exposed by drilling are as follows: A greyish-brown sandy silt in a depth between 200 and 280 cm (well sorted and maximum in the fine sand fraction and therefore eolian origin). Underneath to 360 cm depth, dark-grey humic clay occurred which was deposited on the former lake bottom (1424.8–1425.6 m a.s.l.). Between 360 and 550 cm depth, grey silty sand of eolian origin occurred again. Down to 600 cm (1422.5 m a.s.l.), water-saturated, stone-rich sandy silt followed. The latter layer might be parallelized with the older fanglomerates on the alluvial fan. Furthermore, it is supposed that this layer would have provided additional water flow into the thufur swamp.

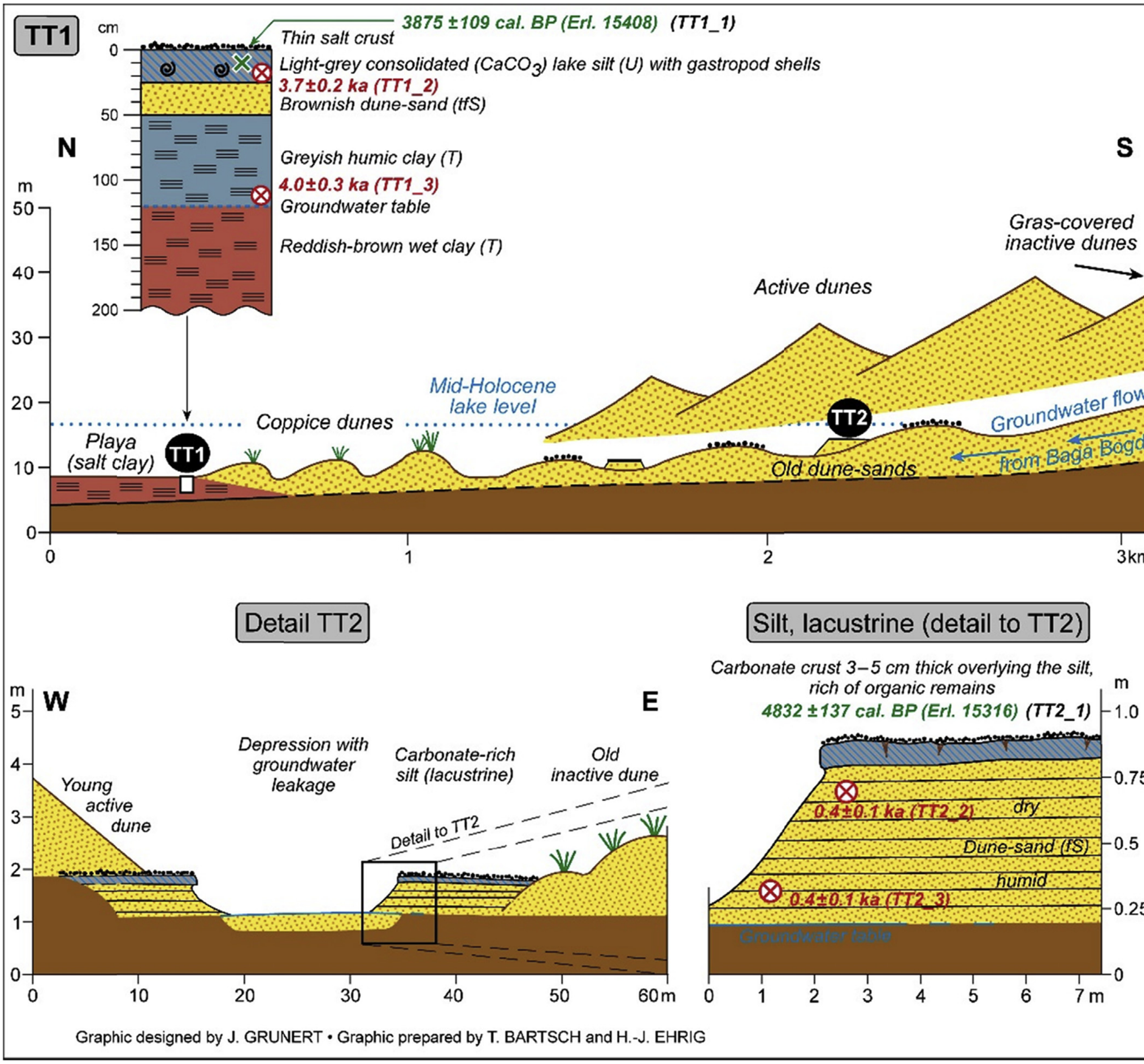

Fig. 8. Cross sections from the Taatsiin Tsagaan Nuur. Carbonate content of the carbonate crust: 8%.

As no absolute dating is available, a supposed connection with the dated fan sediments is uncertain. In BT2 the upper fanglomerate layer is 10 m thick, the dark-grey clay ±9 m and the lower fanglomerate layer 5–6 m above the lake bottom (1417 m a.s.l.). Regarding the OSL age of 12.6 ka (BT1) the upper fanglomerate should have formed contemporaneously with the paleolake-level at 9 m as indicated by the dark-grey clay (BT2). At that time the climate should have been more humid than today. The older (lower) fanglomerate in BT2 has to be connected with a lower paleolake-level, presumably 5–6 m above the lake bottom, indicating a lower lake level and perhaps more arid conditions during the LGM to Late Glacial. The mountain range in the hinterland was not glaciated during the LGM, and reasonable glacial meltwater discharge during the summer did not occur.

The coppice-like dunes have OSL ages of 3.3 ± 0.4 ka, 1.8 ± 0.2 ka and 1.4 ± 0.2 ka, respectively (Fig. 12, Fig. S27, Table 1F and Table S16). Five OSL dates from dune sand at the 9 m level on the southern border of the paleolake all provided young ages <0.2 ka, BT3). Within this partly active dune field representing the most eastern part of the Khongoryn Els, no remnants of old beach ridges could be found.

A core from the Bayan Tohomin Nuur of 7 m length was obtained from the center of the dry lake bottom (Felauer, 2011; Felauer et al., 2012). The predominant sediment is dark-grey silty clay interbedded with layers of fine sand. Eight radiocarbon ages are reported by Felauer et al. (2012). The sediment at 670 cm depth was dated to 12,661 ± 65 cal. BP (BT4_4, Erl-12110). Dates at 520 cm, 350 cm, and 250 cm depths are 6884 ± 64 cal. BP (BT4_3, Erl-13182), 9674 ± 85 cal. BP (BT4_2, Erl-12109) and 6709 ± 45 cal. BP (BT4_1, Erl-13181) respectively. We assume a remobilization of older lake sediments, probably from the sides of the basin at this part of the core. However, considering the complete set of ages a

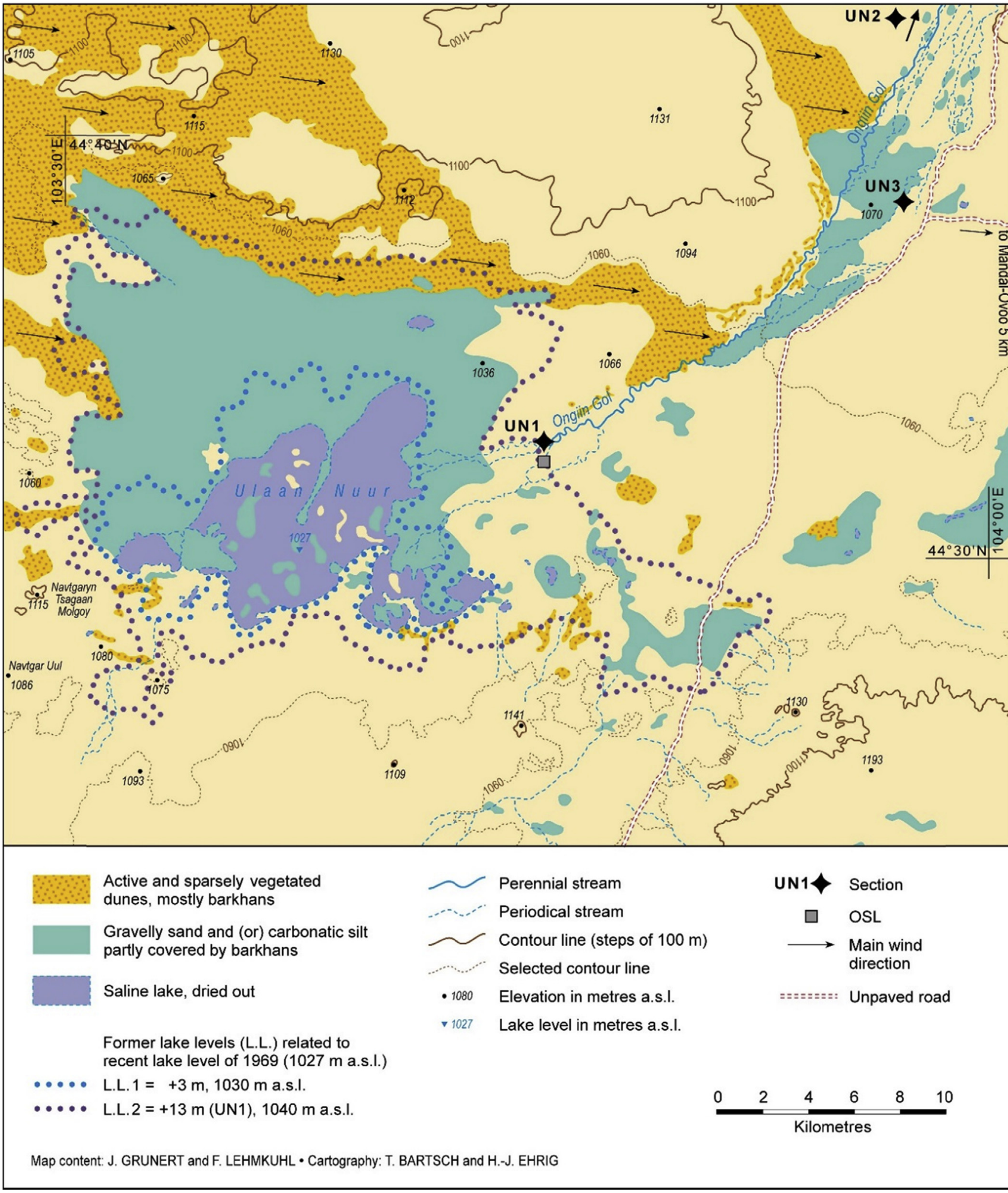

Fig. 9. Map of the Ulaan Nuur depression.

persistent lake during the early Holocene until at least the early-mid Holocene existed.

4.4.2. *Khongoryn Nuur and Khongoryn Els*

The Khongoryn Nuur (1340 m a.s.l.) is located about 70 km west of the Bayan Tohomin Nuur. It is the terminal basin of the Khongoryn Gol, a periodic river on the north side of the up to 60 m high dunes of the Khongoryn Els (Fig. 13). At 15 km upstream, the river crosses the dune field in a meandering valley of only 3 km length. It drains the northern flank of a 2500 m high mountain range 5–6 km

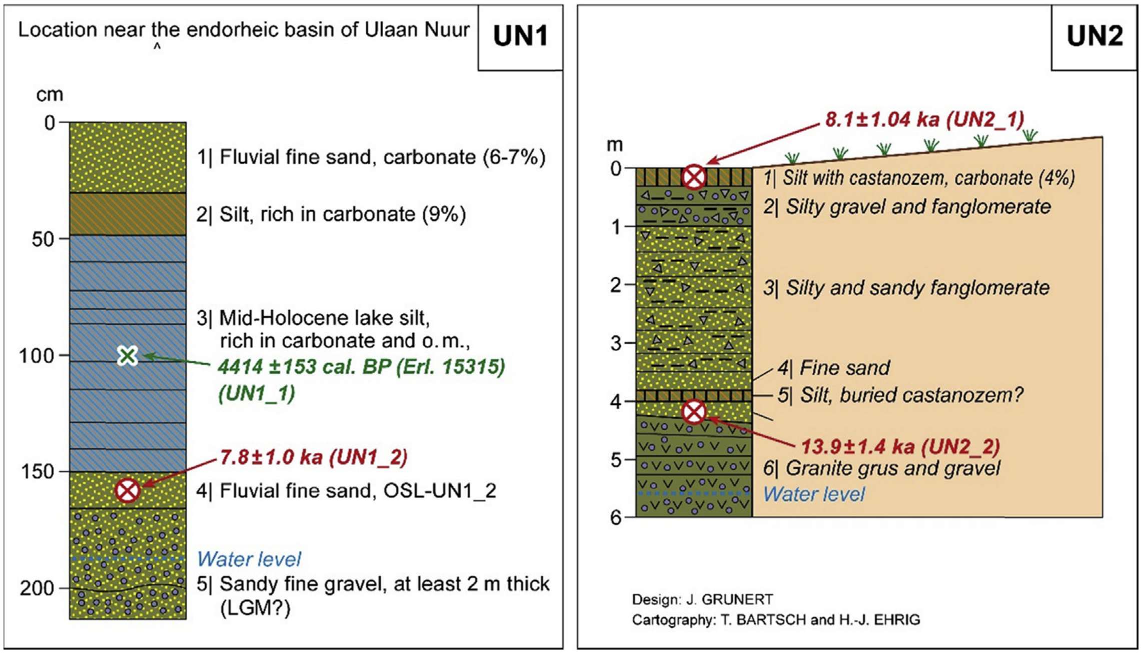

Fig. 10. Sections of the Ongiin Gol valley, lower reaches and middle reaches (UN 1 and UN2).

away from the dune field. Episodic floods of the river are reported; e.g. in the first days in August 2000 during heavy rainfall. Several months later, the usually dry terminal basin had transformed into a lake (Grunert et al., 2009).

3 km upstream of the basin, a profile (KE1 in Fig. 13, 43.81°N, 102.2°E) was studied at a 150 cm high cut-off slope. The sediment sequence is as follows (Hülle, 2011): The upper 15 cm of the section consists of carbonate silty lake sediment. Underneath between 15 and 50 cm depth there is medium-sized sand, followed again by silty lake sediments (between 50 and 60 cm). Down to 150 cm depth, fine eolian sand was observed.

One sample at 90 cm (KE1_1) was OSL-dated to 6.5 ± 0.5 ka. Consequently, the lake sediments above are younger in age. The shallow lake covered large parts of the central depression north of the dune field (B in Fig. 13).

5 km upstream (see Fig. 14) within a coppice dune field, another cut-off slope of 4 m height was investigated (KE2; Figs. S28 and S29, Table S18). Lacustrine, fluvial and aeolian sediments were interbedded (Hülle, 2011). Eolian sand below lake (playa) sediments was OSL-dated to 22.6 ± 1.6 ka (KE2_1, Hülle, 2011). The lacustrine deposits are presumably of Holocene age.

4.4.3. Ujim Sair and surroundings

Ujim Sair (KE3, 1486 m a.s.l.; Figs. S30 and S31) is situated at the entrance into the dune field, 15 km east of the terminal basin. The Khongoryn Gol has been periodically dammed by dunes encroaching this valley (see Fig. 13 A). This is evidenced by a 23 m high sediment sequence formed by thick dune sand and thin clayey layers representing playa-like deposits (Hülle et al., 2010). The dune sand at 20 m depths near the base was dated to 27.1 ± 2.6 ka (KE3_3, Hülle et al., 2010, Table 1G). 10 ages from the sand layers interbedded with playa sediments gave all ages around 15 ka, suggesting a quick sedimentation within a short period during the Late Glacial. Contemporaneously, dunes encroaching at Ujim Sair have dammed episodic floods of the river. This is impossible under modern climate conditions as shown during the large flood in August 2000, when few meters high dunes, which had partly encroached the valley, were completely eroded. During the playa-stage the climate must have been, therefore, more arid and windy than today. This was a large contrast compared with the relatively humid climate conditions during the mid-Holocene, which were favorable for lake formation in the lower parts of the basin (phase B in Fig. 13), and when the dunes were probably fixed by vegetation while sand encroaching towards the valley was impossible.

About several 100 m southeast of section Ujim Sair (KE3) the exposure KE4 (1510 m a.s.l.; 43.75°N, 102.37°E, Figs. 13 and 14; Tables S19 and S20) in a small gully at the distal part of an alluvial fan originating from the mountain range to the south showed deposition of gravel interrupted by some thin silt layers (Fig. 14). The silt layer in 325–350 cm shows small involutions and ice wedge cast features in the upper part (340 cm). The OSL sample from 350 cm depth provided an age of 11.5 ± 1.2 ka (KE2, see Fig. 14). This indicates that the ice wedge casts originated in the Younger Dryas period followed by accumulation of fanglomerates layers from sheet flows and debris flow as a result of active fluvial dynamics during the Holocene. Fluvial erosion is supposed to have been strong enough keeping the dune valley of Ujim Sair permanently free from dune encroachment during that time.

5. Discussion

The eight lakes from the Valley of the Great Lakes and the Valley of the Gobi Lakes described and interpreted in the frame of this study experienced several phases of lake level high-stands during the late Quaternary. However, there are distinct differences between the lakes, especially regarding the timing of high lake levels in the Holocene.

5.1. MIS 5e and MIS 3

High lake levels during the last interglacial (MIS 5e) were directly dated at two lakes, the Zavkhan Gol and the Taatsiin Tsagaan Nuur (Fig. 15). At the Zavkhan Gol a lake of 17 m depth and with an area of nearly 600 km^2 was reconstructed. This lake did not exist during the MIS 6. At the Taatsiin Tsagaan Nuur the lake level at

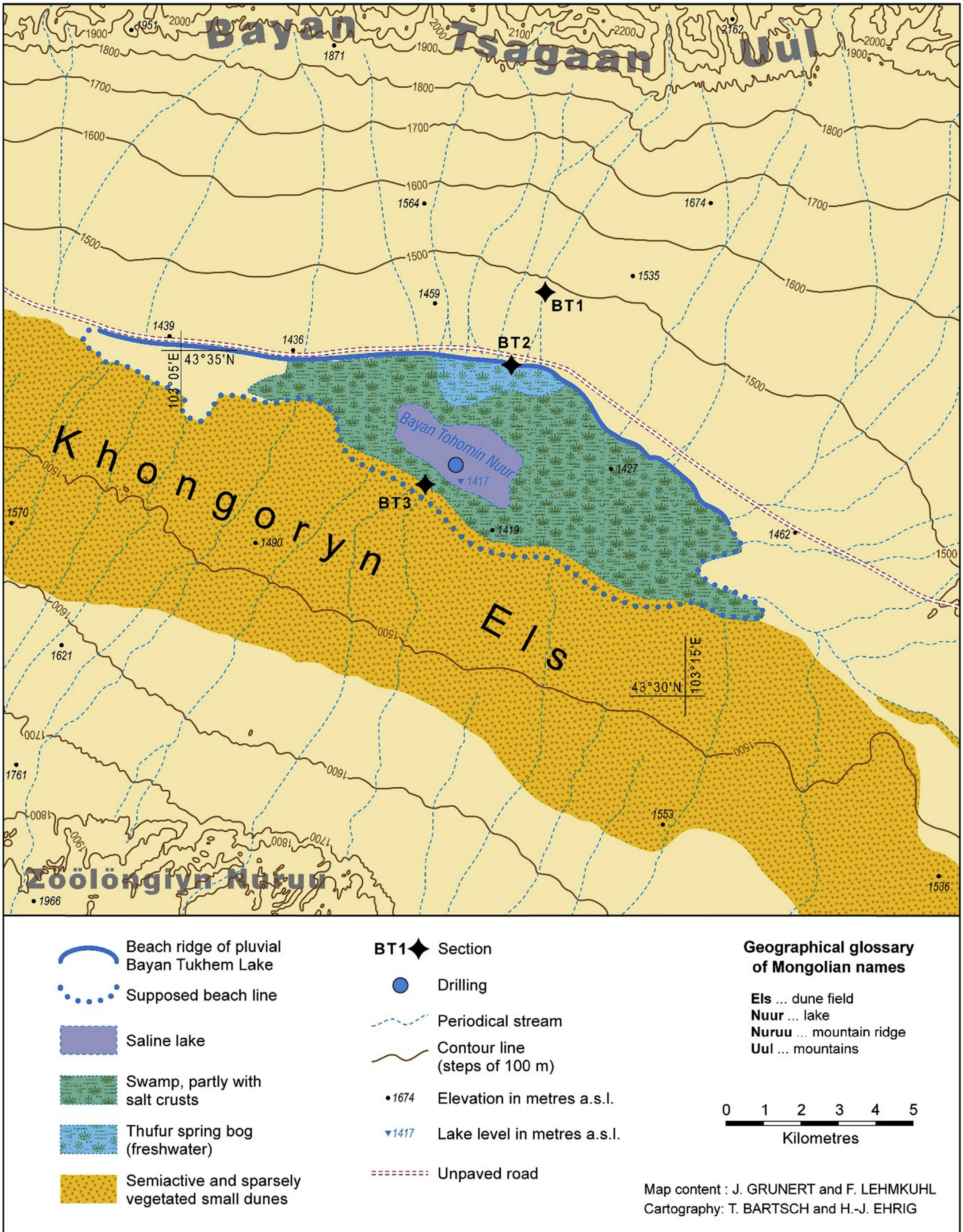

Fig. 11. Map of the Bayan Tohomin Nuur depression. Results of the drilling are published by Felauer et al. (2012).

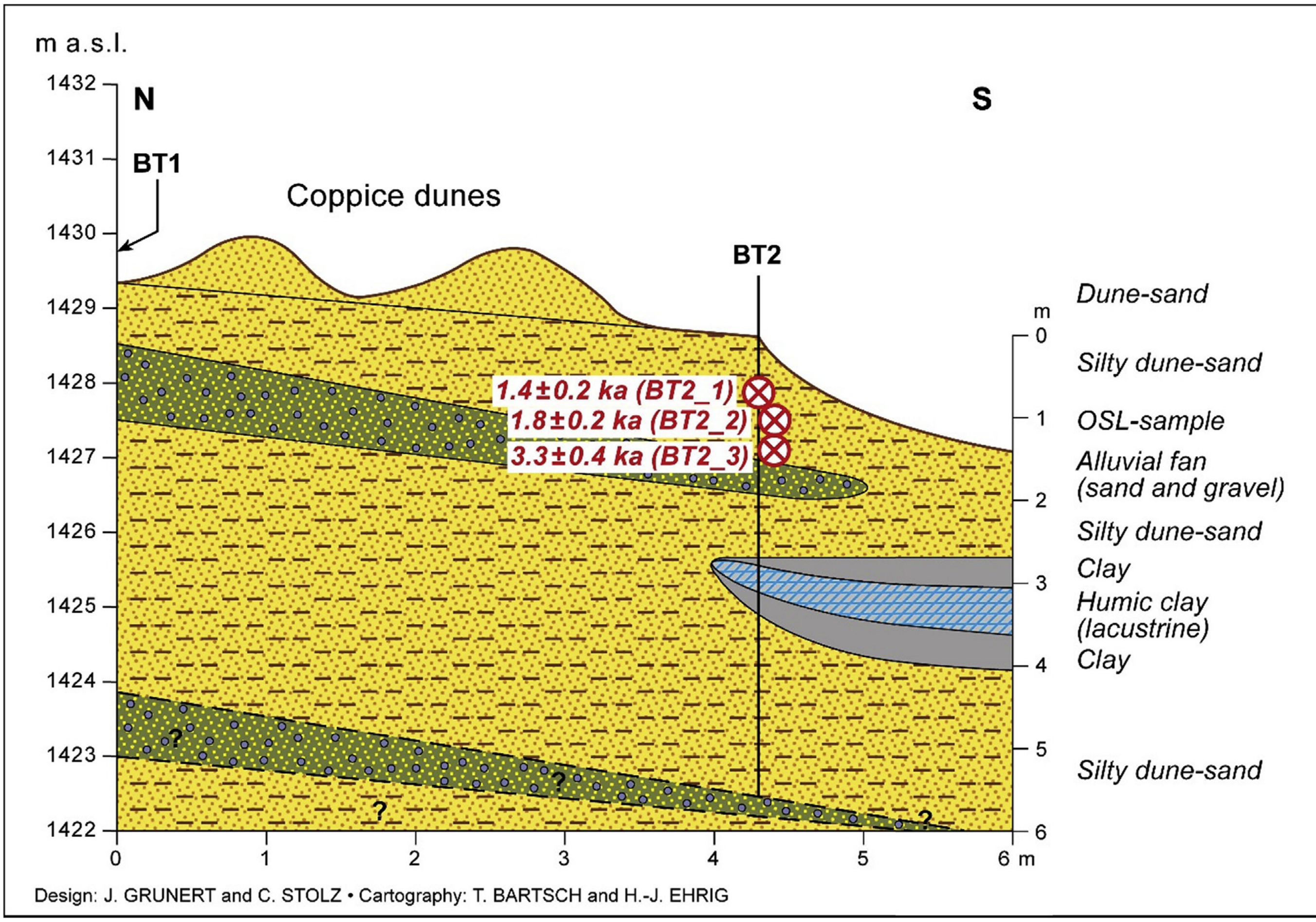

Fig. 12. Section on the northern bank of the Bayan Tohomin Nuur.

that time was 40–43 m above the present one. At the Orog Nuur a lake level 60 m above the present was dated to 70 to 80 ka. As the two latter lakes are located close to each other, we assume a similar timing of both lakes, with a lake at the Orog Nuur probably lasting from the MIS 5e to the early part of the last glacial. At the Ulaan Nuur, sand below lake deposits was dated to 162 ka, again showing a dry phase in the MIS 6. No ages are available for the younger lake sediments above, but due to the similar structure of the sediments at the Zavkhan Gol and the high lake levels at the Taatsiin Tsagaan Nuur and probably at the Orog Nuur an MIS 5e age is assumed. The lake in the Ulaan Nuur basin had a depth of ~43 m. In contrast to all other basins, only sediments from the Orog Nuur indicate a significant lake during the MIS 3.

Giant paleolakes during the last interglacial were also described from areas south of Mongolia (e.g. Long and Shen, 2015). Lai et al. (2014) presented for the freshwater "Shell Bar" in the Qaidam Basin new luminescence ages which place this bar into MIS 5 (~113–99 ka), much older than previous radiocarbon ages of 40 ka BP. They attribute the differences to the age limit of radiocarbon ages. Li et al. (2015) provide new luminescence dating results for the Juyanze Basin in the central Gobi Desert of China. A buried shoreline ~33 m above the basin floor was dated to a time span from ~122 to 73 ka suggesting a 1800 km^2 paleolake during this time. Long et al. (2015) combined OSL and radiocarbon ages from a sediment core from Xingkai Lake, NE China. The comparison of OSL and ^{14}C ages suggested that the radiocarbon dating results significantly underestimate the age of sediments for samples older than 30 cal ka BP.

High lake levels in western and southern Mongolia were caused by a significant wetter climate. High insolation values during the MIS 5e (Fig. 15) resulted in an enhanced land-ocean contrast and a stronger monsoonal circulation (Wang et al., 2008). A strengthening of the monsoonal system during this time is also indicated by smaller grain sizes in the Chinese Loess Plateau (Sun et al., 2006). A weaker winter monsoon and a denser vegetation cover in northern China resulted in a considerable smaller grain size compared to phases with an intensive winter monsoon (Fig. 15). During the MIS 5e the Asian summer monsoon presumably reached southern and western Mongolia, resulting in the formation of large lakes. In contrast, the Asian summer monsoon was much weaker during the MIS 3 than during the MIS 5e (Fig. 15; Wang et al., 2008). Higher lake levels at the Orog Nuur were probably caused by an enhanced meltwater inflow from the Khangai Mountains. Rother et al. (2014) and Lehmkuhl et al. (2016) described a significant ice advance during the MIS 3 in the Khangai Mountains, which was not reported for other areas in Mongolia.

5.2. Lake levels during the MIS 2

Previous studies assumed high lake levels during phases of extensive glaciations (Deviatkin et al., 1987). Glaciations in the presently arid to semi-arid climate of Mongolia require a considerable amount of precipitation (Rother et al., 2014; Lehmkuhl et al., 2016). However, while Lehmkuhl et al. (2011, 2016) reported

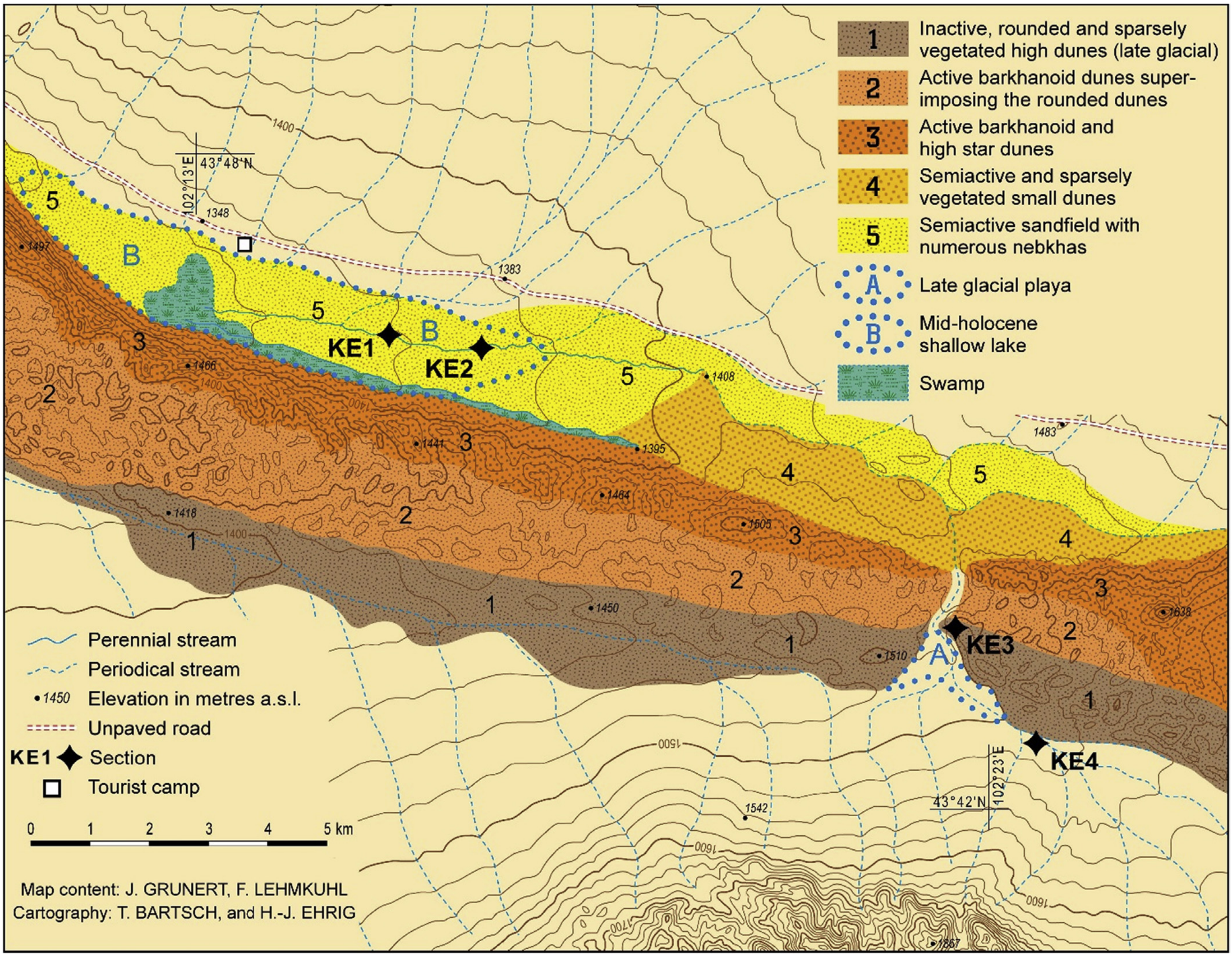

Fig. 13. Map from the central part of the Khongoryn Els.

remnants of considerable ice advantages in the Khangai as well as in the Mongolian Altai during the MIS 2, results from this study indicate low lake levels or even disappearing lakes during this time. Especially at the Zavkhan Gol and the Bayan Tohomin Nuur aeolian sands of MIS 2 ages point to completely dried out lakes. MIS 2 aeolian sands also were reported from the Orog Nuur (Yu et al., 2016, 2017) and the Ulaan Nuur (Lee et al., 2011). Therefore, the previous assumption that high lake levels in the basins of western and southern Mongolia occur in general synchronous to major glaciations in the Altai and Khangai Mountains is not supported by this study.

We found indications for permafrost in the ice wedge cast in section KE4, which is dated to the Late Glacial (11.5 ± 1.2 ka). The undated cryoturbation features (section ZG1, ZG6, UN3, KE2) which occur in the basins can be related to permafrost conditions too. Such features are also described and dated to the Late Glacial by Owen et al. (1998). During the last glacial period there was a southwards shift and lowering of the discontinuous and continuous permafrost conditions (Vandenberghe et al., 2014 and references therein). However, permafrost and periglacial features can also be related to moister and colder periods in the area as periglacial phenomena need humidity and not only temperature depression (Lehmkuhl, 2016). Moreover, a high groundwater level supported this cryturbations.

5.3. Early to mid-Holocene high lake levels

A complex picture emerged from the pattern of high lake levels in the early and mid-Holocene. High lake levels in the early Holocene were recorded at the Zavkhan Gol in the Valley of the Great Lakes. This high-stand occurred from around 9.2 to 7.2 ka. Additional high lake levels were identified at Adagin Tsagaan Nuur, the westernmost basin in the Valley of the Gobi Lakes. In contrast, mid-Holocene high lake levels occurred at the Boon Tsagaan Nuur, the Orog Nuur, the Taatsiin Tsagaan Nuur, the Ulaan Nuur, and the Khongoryn Nuur. However, there has been some considerable debate about the timing of the highest humidity in central Asia (e.g. Chen et al., 2008). Several records indicate a more humid period in the early Holocene and a reduced precipitation in the mid-Holocene in northern China (An et al., 2012; Jin et al., 2015). In contrast, other records indicate an increase in moisture during the early Holocene, but maximum values were reached during the mid-Holocene (Herzschuh, 2006; Wang et al., 2010). This maximum is also consistent with the timing of paleosol formation in the Chinese Loess Plateau (Wang et al., 2014) and the fixation of eolian sediments (Stauch, 2015) on the north-eastern Tibetan Plateau. The

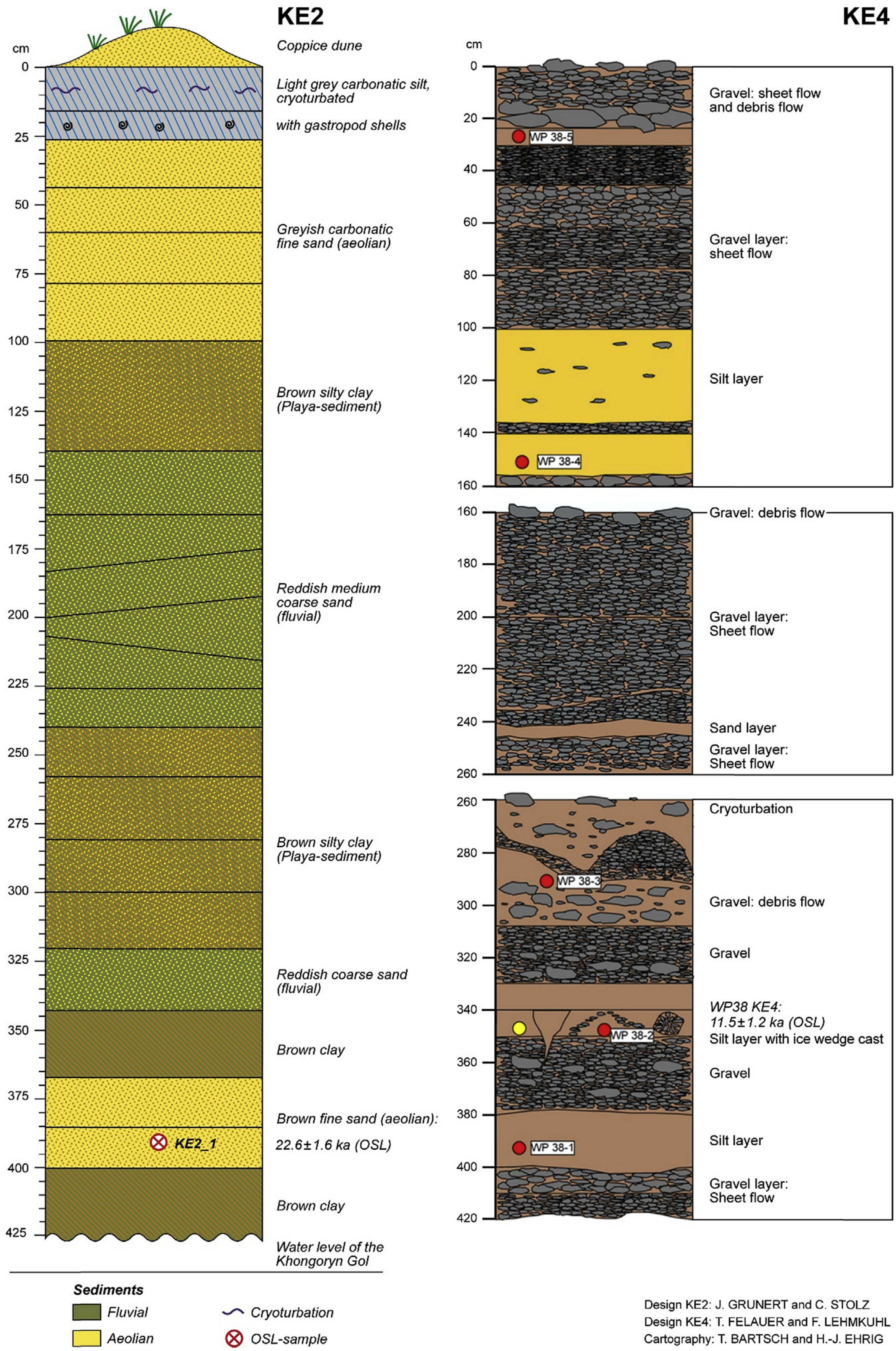

Fig. 14. Section KE2 and section KE4.

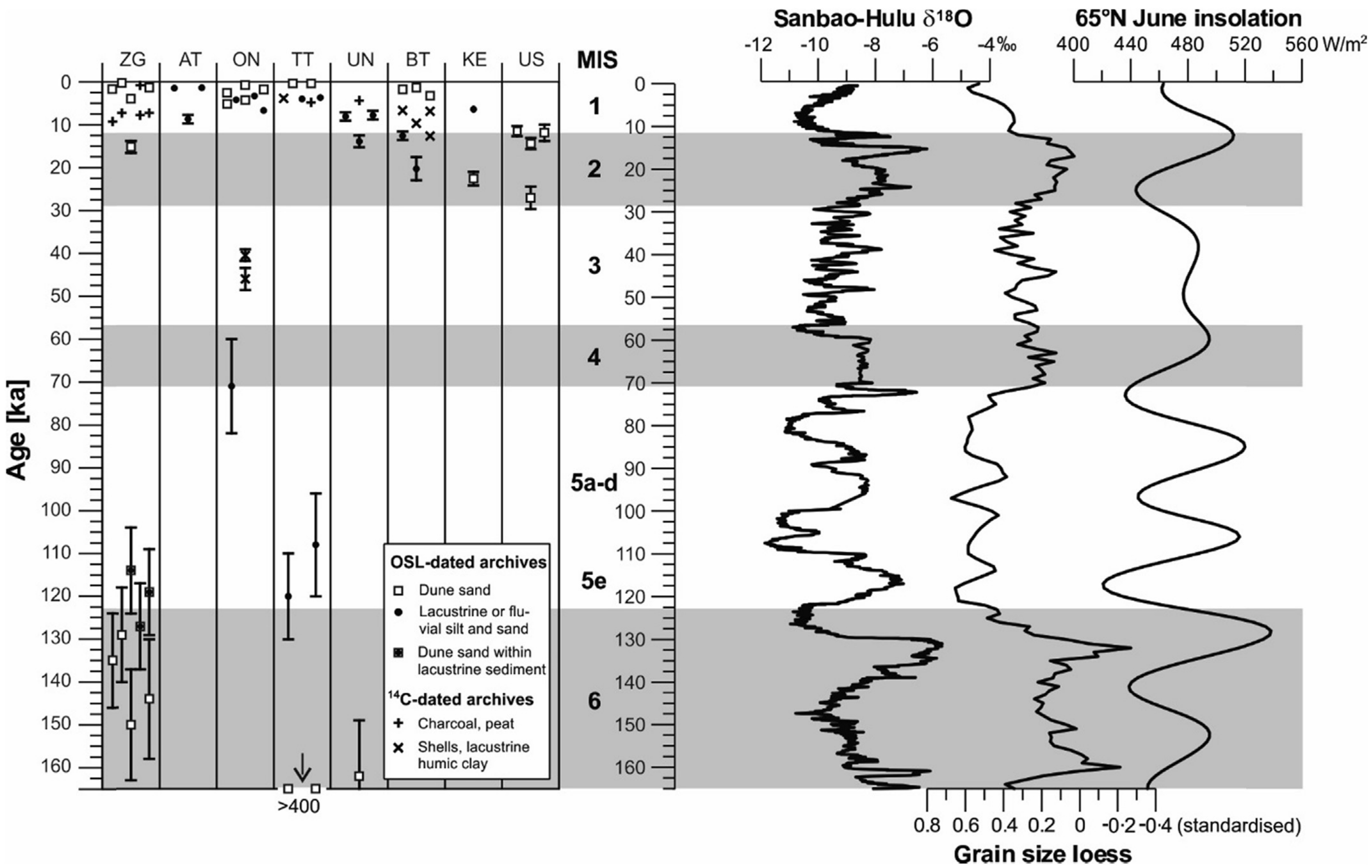

Fig. 15. Luminescence and radiocarbon dating for the last 170 ka and their environment (dated material: OSL and ^{14}C) for the 8 lake basins (see Table 1). For comparison: $\delta^{18}O$ of Sanbao-Hulu cave (Wang et al., 2001, 2008), grain size from the Chinese Loess Plateau (Sun et al., 2006) and June insolation of 65°N (Laskar et al., 2004). Dark grey shades are cold phases.

differences in the moisture evolution between the Zavkhan Gol and the Adagin Tsagaan Nuur and the remaining lakes in southern Mongolia might be caused by different large atmospheric systems. An early Holocene humid period was especially recognized in northern and western Mongolia (Grunert et al., 2000; Naumann and Walther, 2000; Walther et al., 2003; Grunert and Dash, 2004; An et al., 2008; Watanabe et al., 2009; Lehmkuhl et al., 2011, 2012). Tarasov et al. (2000) investigated the lake Hoton Nuur in the westernmost part of Mongolia and assumed an onset of wetter climate conditions before 9 ka. An even earlier onset was reported from the Gun Nuur on the northern Mongolian Plateau. The phase of highest humidity at the Gun Nuur occurred from 10.3 ka until 7 ka (Zhang et al., 2012). In the Shaamar eolian section a well-developed paleosol indicates early Holocene humid conditions (Feng et al., 2006).

In contrast, most records from southern Mongolia and northern China indicate higher humidity in the mid-Holocene (e.g. Feng et al., 2006). A pollen record from Gonghai Lake in northern China indicates an intensified monsoon in the mid-Holocene with highest precipitation values from 7.8 to 5.3 ka (Chen et al., 2015). A similar timing was described for Daihai Lake (Xiao et al., 2004) and Dali Lake (Xiao et al., 2008). This was related to the northward movement of the East Asian Summer Monsoon (Xiao et al., 2008). However, at Dali Lake highest lake levels occurred in the early Holocene. While Xiao et al. (2008) assumed an enhanced meltwater inflow during this time, Goldsmith et al. (2017) assumed an early Holocene precipitation maximum. Similar contradicting results were reported from the Ugii Nuur in central Mongolia. While Wang et al. (2011) assumed a dry mid-Holocene climate; Schwanghart et al. (2009) reconstructed wet climate conditions for this period. At the Ulaan Nuur Lee et al. (2013), based on a sediment core, suggest more humid conditions in the early Holocene. However, the data from this study supports high lake levels in the mid-Holocene. The mid-Holocene precipitation maximum can be related to a strengthening of the EASM, which reached at least southern Mongolia during that time. The early Holocene humid period in western Mongolia is comparable to a warming trend in the north of Mongolia (An et al., 2008) and might be related to a stronger influence of the mid-latitude westerlies in the area, which are probably stronger influenced by insolation changes than the EASM.

5.4. Late Holocene lake levels

In addition, the data suggest a dry Late Holocene with more active dunes (Fig. 15). Despite that, lake levels of late Holocene age are documented from the Zavkhan Gol, the basins of Boon Tsagaan Nuur, Adagin Tsagaan Nuur and the Orog Nuur. However, these lake levels were much lower than during the previous periods. Higher than present lake levels were also previously recorded in western Mongolia (e.g. Peck et al., 2002; Fowell et al., 2003). In most studies from southern Mongolia and northern China the late Holocene is characterized by distinct drier climate conditions (Chen et al., 2015, 2016; Stauch, 2016). The Daihai Lake (Xiao et al., 2004) and Gonghai Lake (Chen et al., 2015) experienced drier climate conditions than the mid-Holocene since 4.5 ka and 3.3 ka, respectively. The late Holocene trend of less humid conditions in southern Mongolia was caused by the southward retreat of the EASM. However, also a stronger human impact with overgrazing occurred in this period (Schlütz and Lehmkuhl, 2007, 2009; Lehmkuhl et al., 2011, 2012). Furthermore, many lakes disappeared during the 20th century. This can also be attributed to an increased human influence in the area and the increased consumption of water.

6. Conclusion and outlook

Highest lake levels occurred during the last interglacial (MIS 5e). During this period, large paleolakes covered extended parts of the basins. This important lake period was previously unknown in southwestern Mongolia. Higher insolation values resulted in a significant stronger Asian summer monsoon, bringing moisture far into Mongolia. Only at one lake, higher lake levels during the MIS 3 are evident. However, they were probably not related to higher precipitation values but to the higher input of melt water from the nearby Khangai Mountains. Holocene lake level variations indicate a complex picture. While two lakes at the western end of the study area experienced high lake levels in the early Holocene, most other lakes have a Holocene maximum in the mid-Holocene. This difference might by caused by varying moisture bearing air masses in the area. Lakes in western Mongolia experienced higher lake levels during the early Holocene, probably caused by enhanced westerlies due to higher insolation values. The lakes in southern Mongolia had higher lake levels in the mid-Holocene due to the influence of the EASM. This assumption is in accordance with many recent results from northern China. During the late Holocene many lakes experienced lower lake levels. All basins investigated in this study are suffering from severe desiccation since 1960. Shallow but perennial lakes have disappeared within 50 years except the brackish Boon Tsagaan Nuur. This is caused by an enhanced human influence.

Acknowledgements

We are greatly thankful to the German Research Foundation (DFG, LE 730/16-1, GR 597/15-1, RA383/16-1) for the financial support to carry out two expeditions of several weeks each in a scientifically important but remote area of Mongolia. Our warmest thanks include the members of the Geographical Institute of the Mongolian Academy of Science in Ulaanbaatar especially the director Prof. Dr. Dordjgotov for the broad logistical support. Thanks to the PhD-students of the National University of Mongolia in Ulaanbaatar who assisted at the fieldwork, and, not forget the excellent teamwork during several weeks in the field under harsh conditions. In addition, field work, analysis and numerous discussions were supported by C. Stolz (Mainz University) and two former PhD-Students: T. Felauer (RWTH Aachen University) and N. Hempelmann (Mainz University). V. Niedek (RWTH Aachen University) helped to compile the supplement data, T. Bartsch (Mainz) and A. Ehrig (RWTH Aachen University) draw most of the figures. V. Nottebaum, W. Römer, Kaifeng Yu and C. Zeeden helped with several discussions and valuable comments on the first draft of the paper. Special thanks to A. Hilgers (former head of the luminescence laboratory of the University of Cologne) for her great effort in sampling in Mongolia and doing much of the dating in Cologne. In addition, we would like to thank Xiaoping Yang as editor and two anonymous reviewers who helped to improve the paper.

Appendix A. Supplementary data

Supplementary data related to this article can be found at https://doi.org/10.1016/j.quascirev.2017.10.035.

References

Academy of Sciences of Mongolia and Academy of Sciences of USSR, 1990. National Atlas of the Peoples Republic of Mongolia. Ulaan Baatar, Moscow.

An, C., Chen, F., Barton, L., 2008. Holocene environmental changes in Mongolia: a review. Glob. Planet. Change 63, 283–289.

An, Z., Colman, S.M., Zhou, W., Li, X., Brown, E.T., Jull, A.J.T., Cai, Y., Huang, Y., Lu, X., Chang, H., Song, Y., Sun, Y., Xu, H., Liu, W., Jin, Z., Liu, X., Cheng, P., Liu, Y., Ai, L., Li, X., Liu, X., Yan, L., Shi, Z., Wang, X., Wu, F., Qiang, X., Dong, J., Lu, F., Xu, X., 2012. Interplay between the Westerlies and Asian monsoon recorded in lake Qinghai sediments since 32 ka. Sci. Rep. 2, 619.

Aitken, M.J., 1998. An Introduction to Optical Dating. Oxford University Press, Oxford.

Auclair, M., Lamothe, M., Huot, S., 2003. Measurement of anomalous fading for feldspar IRSL using SAR. Radiat. Meas. 37, 487–492.

Baljinaym, I., Bayasgalan, A., Brorisov, B.A., Cisternas, A., Dem'yanovich, M.G., Ganbaatar, L., Kochetkov, V.M., Kurushin, R.A., Molnar, P., Herve, P.H., Vashchilov, Y.Y., 1993. Ruptures of major earthquakes and active deformation in Mongolia and its surroundings. Mem. Geol. Soc. Am. 181.

Berkey, C.P., Morris, K.K., 1927. Geology of Mongolia. Am. Mus. Nat. Hist. New York.

Bøtter-Jensen, L., McKeever, S.W.S., Wintle, A.G., 2003. Optically Stimulated Luminescence Dosimetry. Elsevier, Amsterdam.

Buylaert, J.P., Murray, A.S., Thomsen, K.J., Jain, M., 2009. Testing the potential of an elevated temperature IRSL signal from K-feldspar. Radiat. Meas. 44, 560–565.

Chen, F., Yu, Z., Yang, M., Ito, E., Wang, S., Madsen, D.B., Huang, X., Zhao, Y., Sato, T., Birks, H.J.B., Boomer, I., Chen, J., An, C., Wünnemann, B., 2008. Holocene moisture evolution in arid central Asia and its out-of-phase relationship with Asian monsoon history. Quat. Sci. Rev. 27, 351–364.

Chen, F., Xu, Q., Chen, J., Birks, H.J.B., Liu, J., Zhang, S., Jin, L., An, C., Telford, R.J., Cao, X., Wang, Z., Zhang, X., Selvaraj, K., Lu, H., Li, Y., Zheng, Z., Wang, H., Zhou, A., Dong, G., Zhang, J., Huang, X., Bloemendal, J., Rao, Z., 2015. East Asian summer monsoon precipitation variability since the last deglaciation. Sci. Rep. 5, 11186.

Chen, F., Wu, D., Chen, J., Zhou, A., Yu, J., Shen, J., Wang, S., Huang, X., 2016. Holocene moisture and East Asian summer monsoon evolution in the northeastern Tibetan Plateau recorded by Lake Qinghai and its environs: a review of conflicting proxies. Quat. Sci. Rev. 154, 111–129.

Devjatkin, E.V., 1981. Cenozoic of Inner Asia. Nauka, Moskow [in Russian].

Deviatkin, E.V., Saitzew, N.S., Kurina, N.A., Florensow, N.A., Korschnew, S.S., 1987. Geomorphological map of socialist Mongolian Republic, 1, 1,5 Mio. Moscow. (in Russian).

Dinesman, L.G., Kiseleva, N.K., Knyazev, A.B., 1989. History of Steppe Ecosystem of Mongolia. Nauka, Moscow, p. 204 (in Russian).

Dorofeyuk, N.I., 2008. Reconstruction of Nature Conditions of Central Asia in Late Glacial and Holocene (Material of Diatom and Palinological Analyses of Lake Sediments of Mongolia). Autoreferat of dissertation of doctor PhD biological sciences. Moscow, p. 43 (in Russian).

Felauer, T., 2011. Jungquartäre Landschafts- und Klimageschichte der Südmongolei. Dissertation an der Fakultät für Georessourcen und Materialtechnik der RWTH Aachen.

Felauer, T., Schlütz, F., Murad, W., Mischke, S., Lehmkuhl, F., 2012. Late Quaternary climate and landscape evolution in arid Central Asia: a multidisciplinary research of lake archive Bayan Tohomin Nuur, Gobi desert, southern Mongolia. J. Asian Earth Sci. 48, 125–135.

Feng, Z.-D., An, C.B., Wang, H.B., 2006. Holocene climatic and environmental changes in the arid and semi-arid areas of China: a review. Holocene 16, 119–130.

Fowell, S.J., Hansen, B.C.S., Peck, J.A., Khosbayar, P., Ganboöd, E., 2003. Mid to late Holocene climate evolution of the Lake Telmen Basin, North Central Mongolia, based on palynological data. Quat. Res. 59, 353–363.

Geodesy and Cartography Agency of Mongolia, 1978. Topographic Map of Mongolia. Scale 1, 500,000. Ulaanbaatar.

Goldsmith, Y., Broecker, W.S., Xu, H., Polissar, P.J., deMenocal, P.B., Porat, N., Lan, J., Cheng, P., Zhou, W., An, Z., 2017. Northward extent of East Asian monsoon covaries with intensity on orbital and millennial timescales. Proc. Natl. Acad. Sci. https://doi.org/10.1073/pnas.1616708114.

Grunert, J., Dash, D., 2004. Dynamics and evolution of dune fields on the northern rim of the Gobi Desert (Mongolia). Z. für Geomorphol. N.F. Suppl. 133, 81–106.

Grunert, J., Stolz, C., Hempelmann, N., Hilgers, A., Hülle, D., Lehmkuhl, F., Felauer, T., Dasch, D., 2009. The evolution of small lake basins in the Gobi desert in Mongolia. Quat. Sci. 29, 678–686.

Grunert, J., Lehmkuhl, F., 2004. Aeolian sedimentation in arid and semi-arid environments of Western Mongolia. In: Smykatz-Kloss, W., Felix-Henningsen, P. (Eds.), Paleoecology of Quaternary Drylands. Lecture Notes in Earth Sciences 102. Springer, Berlin, Heidelberg, pp. 195–218.

Grunert, J., Lehmkuhl, F., Walther, M., 2000. Paleoclimatic evolution of the Uvs Nuur basin and adjacent areas (Western Mongolia). Quat. Int. 65/66, 171–192.

Herzschuh, U., 2006. Palaeo-moisture evolution in monsoonal Central Asia during the last 50,000 years. Quat. Sci. Rev. 25, 163–178.

Hülle, D., 2011. Lumineszenzdatierung von Sedimenten zur Rekonstruktion der jungquartären Landschaftsentwicklung in der Mongolei. Dissertation an der Mathematisch-Naturwissenschaftlichen Fakultät der Universität zu Köln.

Hülle, D., Hilgers, A., Radtke, U., Stolz, C., Hempelmann, N., Grunert, J., Felauer, T., Lehmkuhl, F., 2010. OSL dating of sediments from the Gobi desert, Southern

Mongolia. Quat. Geochronol. 5, 107–113.
Huntley, D.J., Baril, M.R., 1997. The K content of the K-feldspars being measured in optical dating or in thermoluminescence dating. Anc. TL 15, 11–13.
Huntley, D.J., Lamothe, M., 2001. Ubiquity of anomalous fading in K-feldspars, and the measurement and correction for it in optical dating. Can. J. Earth Sci. 38, 1093–1106.
Jin, M., Li, G., Li, F., Duan, Y., Wen, L., Wei, H., Yang, L., Fan, Y., Chen, F., 2015. Holocene shorelines and lake evolution in Juyanze Basin, southern Mongolian Plateau, revealed by luminescence dating. Holocene 25, 1898–1911.
Khosbayar, P., 2005. Mesozoic and Cenozoic Paleogeography and Paleoclimate of Mongolia. Mongolian Academy of Sciences. Institute of Geology and Mineral Resources of Mongolia, Ulaanbaatar, p. 156 (in Mongolian).
Komatsu, G., Brantingham, P.J., Olsen, J.W., Baker, V.R., 2001. Paleoshoreline geomorphology of Boon Tsagaan Nuur, Tsagaan Nuur and Orog Nuur: the valley of lakes, Mongolia. Geomorphology 39, 83–98.
Kurushin, A., Bayasgalan, A., Ölzibat, M., Enhtuvshin, B., Molnar, P., Bayarsayhan, C., Hudnut, K.W., Lin, J., 1997. The Surface Rupture of the 1957 Gobi-altay, Mongolia, Earthquake, vol. 320. Geology Society of America, pp. 1–143. Special Paper.
Lai, Z.P., Mischke, S., Madsen, D., 2014. Paleoenvironmental implications of new OSL dates on the formation of the “shell bar” in the Qaidam Basin, northeastern Qinghai-Tibetan plateau. J. Paleolimnol. 51, 197–210.
Laskar, J., Robutel, P., Joutel, F., Gastineau, M., Correia, A.C.M., Levrard, B., 2004. A long-term numerical solution for the insolation quantities of the Earth. Astron. Astrophys. 428, 261–285. https://doi.org/10.1051/0004-6361:20041335.
Lee, M.K., Lee, Y.I., Lim, H.S., Lee, J.I., Choi, J.H., Yoon, H.I., 2011. Comparison of radiocarbon and OSL dating methods for a Late Quaternary sediment core from Lake Ulaan, Mongolia. J. Paleolimnol. 45, 127–135.
Lee, M.K., Lee, Y.I., Lim, H.S., Lee, J.I., Yoon, H.I., 2013. Late Pleistocene-Holocene records from Lake Ulaan, southern Mongolia: implications for East Asian palaeomonsoonal climate changes. J. Quat. Sci. 28, 370–378.
Lehmkuhl, F., 1998. Quaternary glaciations in central and Western Mongolia. Quat. Proc. 6, 153–167.
Lehmkuhl, F., 2016. Modern and past periglacial features in Central Asia and their implication for paleoclimate reconstructions. Prog. Phys. Geogr. 40, 369–391.
Lehmkuhl, F., Haselein, F., 2000. Quaternary palaeoenvironmental change on the Tibetan Plateau and adjacent areas (Western China and Mongolia). Quat. Int. 65/66, 121–145.
Lehmkuhl, F., Hilgers, A., Fries, S., Hülle, D., Schlütz, F., Shumilovskikh, L., Felauer, T., Protze, J., 2011. Holocene geomorphological processes and soil development as indicator for environmental change around Karakorum, Upper Orkhon Valley (Central Mongolia). Catena 87, 31–44.
Lehmkuhl, F., Hülle, D., Knippertz, M., 2012. Holocene geomorphic processes and landscape evolution in the lower reaches of the Orkhon Valley (northern Mongolia). Catena 98, 17–28.
Lehmkuhl, F., Klinge, M., Rother, H., Hülle, D., 2016. Distribution and timing of Holocene and Pleistocene glacier fluctuations in western Mongolia. Ann. Glaciol. 57 (71), 169–178.
Lehmkuhl, F., Lang, A., 2001. Geomorphological investigations and luminescence dating in the southern part of the Khangay and the Valley of the Gobi Lakes (Mongolia). J. Quat. Sci. 16, 69–87.
Li, G., Jin, M., Duan, Y., Madsen, D.B., Li, F., Yang, L., Wei, H., Chen, F., 2015. Quartz and K-feldspar luminescence dating of a marine isotope stage 5 megalake in the Juyanze Basin, central Gobi desert, China. Palaeogeogr. Palaeoclimatol. Palaeoecol. 440, 96–109.
Lockot, G., Ramisch, A., Wünnemann, B., Hartmann, K., Haberzettl, T., Chen, H., Diekmann, B., 2016. A process- and provenance-based attempt to unravel inconsistent radiocarbon chronologies in lake sediments: an example from lake Heihai, North Tibetan plateau (China). Radiocarbon 57, 1003–1019.
Long, H., Shen, J., 2015. Underestimated ^{14}C-based chronology of late Pleistocene high lake-level events over the Tibetan Plateau and adjacent areas: evidence from the Qaidam Basin and Tengger Desert. Sci. China Earth Sci. 58, 183–194.
Long, H., Lai, Z., Wang, N., Zhang, J., 2011. A combined luminescence and radiocarbon dating study of Holocene lacustrine sediments from arid northern China. Quat. Geochronol. 6, 1–9.
Long, H., Shen, J., Wang, Y., Gao, L., Frechen, M., 2015. High-resolution OSL dating of a late Quaternary sequence from Xingkai Lake (NE Asia): chronological challenge of the “MIS 3a Mega-paleolake” hypothesis in China. Earth Planet. Sci. Lett. 428, 281–292.
Mischke, S., Weynell, M., Zhang, C., Wiechert, U., 2013. Spatial variability of 14C reservoir effects in Tibetan Plateau lakes. Quat. Int. 313–314, 147–155.
Murzaev, E.M., 1954. Die Mongolische Volksrepublik. Physisch-geographische Beschreibung. Gotha.
Murray, A.S., Wintle, A.G., 2000. Luminescence dating of quartz using an improved single-aliquot regenerative-dose protocol. Radiat. Meas. 32, 57–73.
Naumann, S., Walther, M., 2000. Mid-Holocene lake-level fluctuations of Bajan Nuur (North-west Mongolia). Marbg. Geogr. Schriften 135, 15–27.
Owen, L.A., Windley, B.F., Cunningham, W.D., Badamgarov, G., Dorjnamjaa, D., 1997. Quaternary alluvial fans in the Gobi Desert, southern Mongolia: evidence for neotectonics and climate change. J. Quat. Sci. 12, 239–252.
Owen, L.A., Richards, B., Rhodes, E.J., Cunningham, W.D., Windley, B.F., Badamgarov, J., Dorjnamjaa, D., 1998. Relic permafrost structures in the Gobi of Mongolia: age and significance. J. Quat. Sci. 13, 539–547.
Peck, J.A., Khosbayar, P., Fowell, S.J., Pearce, R.P., Ariunbileg, S., Hansen, B.C.S., Soninkhishig, N., 2002. Mid to late Holocene climate change in north central Mongolia as recorded in the sediments of lake Telmen. Palaeogeogr. Palaeoclimatol. Palaeoecol. 183, 135–153.
Prescott, J.R., Hutton, J.T., 1994. Cosmic ray contribution to dose rates for luminescence and ESR dating: large depths and long-term variations. Radiat. Meas. 23, 497–500.
Preusser, F., Degering, D., Fuchs, M., Hilgers, A., Kadereit, A., Klasen, N., Krbetschek, M., Richter, D., Spencer, J., 2008. Luminescence dating: basics, methods and applications. Quat. Sci. J. 57, 95–149.
Rother, H., Lehmkuhl, F., Fink, D., Nottebaum, V., 2014. Timing of late Pleistocene glaciations in the Khangai mountains of Mongolia: evidence for a MIS 3 glacial maximum. Quat. Res. 82, 297–308.
Schlütz, F., Lehmkuhl, F., 2007. Climatic change in the Russian Altai, southern Siberia, based on palynological and geomorphological results with implications on climatic teleconnections and human history since the middle Holocene. Veg. Hist. Archaeobotany 16, 101–116.
Schlütz, F., Lehmkuhl, F., 2009. Holocene climatic change and the nomadic anthropocene in eastern Tibet: palynological and geomorphological results from the Nianbaoyeze mountains. Quat. Sci. Rev. 28, 1449–1471.
Stauch, G., 2015. Geomorphological and palaeoclimate dynamics recorded by the formation of aeolian archives on the Tibetan Plateau. Earth Science Rev. 150, 393–408.
Stauch, G., 2016. Multi-decadal periods of enhanced aeolian activity on the north-eastern Tibet Plateau during the last 2ka. Quat. Sci. Rev. 149, 91–101.
Stolz, C., Hülle, D., Hilgers, A., Grunert, J., Lehmkuhl, F., Dasch, D., 2012. Reconstructing fluvial, lacustrine and aeolian process dynamics in Western Mongolia. Z. für Geomorphol. N. F. 56, 267–300.
Sun, Y., Clemens, S.C., An, Z., Yu, Z., 2006. Astronomical timescale and palaeoclimatic implication of stacked 3.6-Myr monsoon records from the Chinese Loess Plateau. Quat. Sci. Rev. 25, 33–48.
Schwanghart, W., Frechen, M., Kuhn, N.J., Schütt, B., 2009. Holocene environmental changes in the Ugii Nuur basin, Mongolia. Palaeogeogr. Palaeoclimatol. Palaeoecol. 279, 160–171.
Szumińska, D., 2016. Changes in surface area of the Böön Tsagaan and Orog lakes (Mongolia, Valley of the Lakes, 1974–2013) compared to climate and permafrost changes. Sediment. Geol. 340, 62–73.
Tarasov, P.E., Harrison, S.P., 1998. Lake status from the former Soviet Union and Mongolia: a continental-scale synthesis. Palaeoclim. Res. 25, 115–130.
Tarasov, P.E., Peyron, O., Guiot, J., Brewer, S., Volkowa, V.D., Bezusko, L.G., Dorofeyuk, N.J., Kvavadze, E.V., Psipova, J.M., Panova, N.K., 1999. Last glacial maximum climate of the former Soviet Union and Mongolia reconstructed from pollen and plant macrofossil data. Clim. Dyn. 15, 227–240.
Tarasov, P., Dorofeyuk, N., Sevastyanov, D., Nakagawa, T., 2000. Holocene vegetation and climate changes in Mongolia derived from lake status, pollen and plant macrofossil records. Berl. Geowiss. Abh. A 205, 94–99.
Thiel, C., Buylaert, J.P., Murray, A.S., Terhorst, B., Hofer, I., Tsukamoto, S., Frechen, M., 2011. Luminescence dating of the Stratzing loess profile (Austria) - Testing the potential of an elevated temperature post-IR IRSL protocol. Quat. Int. 234, 23–31.
Thomsen, K.J., Jain, M., Murray, A.S., Denby, P.M., Roy, N., Bøtter-Jensen, L., 2008. Minimizing feldspar OSL contamination in quartz UV-OSL using pulsed blue stimulation. Radiat. Meas. 43, 752–757.
Vandenberghe, J., French, H.M., Gorbunov, A., Marchenko, S., Velichko, A.A., Jin, H., Cui, Z., Zhang, T., Wan, X., 2014. The Last Permafrost Maximum (LPM) map of the Northern Hemisphere: permafrost extent and mean annual air temperatures, 25–17 ka BP. Boreas 43, 652–666.
Wallinga, J., Murray, A., Wintle, A., 2000. The single-aliquot regenerative-dose (SAR) protocol applied to coarse-grain feldspar. Radiat. Meas. 32, 529–533.
Walther, M., 1998. Paläoklimatische Untersuchungen zur jungpleistozänen Landschaftsentwicklung im Changai-Bergland und in der nördlichen Gobi (Mongolei). Petermanns Geogr. Mittl. 142, 205–215.
Walther, M., 1999. Late Quaternary climate development reconstructed from lake levels in the Uws Nuur basin (NW-Mongolia). Die Erde 130, 131–150.
Walther, M., Enkhjargal, V., Gegeensuvd, Ts, Odbaatar, E., 2016. Environmental changes of Orog Nuur (Bayan Khongor Aimag, South Mongolia) lake deposits, paleo-shorelines and vegetation history. Erforsch. Biol. Ressourcen Mong. 13, 37–57.
Walther, M., Wünnemann, B., Tschimeksaichan, A., 2003. Seen und Paläoseen in der Mongolei und Nordwestchina. Petermanns Geogr. Mittl. 147, 40–47.
Wang, Y.J., Cheng, H., Edwards, R.L., An, Z.S., Wu, J.Y., Shen, C.-C., Dorale, J.A., 2001. A high-resolution absolute-dated late Pleistocene monsoon record from Hulu cave, China. Science 294, 2345–2348.
Wang, Y., Cheng, H., Edwards, R.L., Kong, X., Shao, X., Chen, S., Wu, J., Jiang, X., Wang, X., An, Z., 2008. Millennial- and orbital-scale changes in the East Asian monsoon over the past 224,000 years. Nature 451, 1090–1093.
Wang, Y., Liu, X., Herzschuh, U., 2010. Asynchronous evolution of the indian and East Asian summer monsoon indicated by Holocene moisture patterns in monsoonal central Asia. Earth Sci. Rev. 103, 135–153.
Wang, W., Ma, Y., Feng, Z., Narantsetseg, T., Liu, K.-B., Zhai, X., 2011. A prolonged dry mid-Holocene climate revealed by pollen and diatom records from Lake Ugii Nuur in central Mongolia. Quat. Int. 229, 74–83.
Wang, H., Chen, J., Zhang, X., Chen, F., 2014. Palaeosol development in the Chinese Loess Plateau as an indicator of the strength of the East Asian summer monsoon: evidence for a mid-Holocene maximum. Quat. Int. 334–335, 155–164.
Watanabe, T., Nakamura, T., Watanabe Nara, F., Kakegawa, T., Horiuchi, K., Senda, R.,

Oda, T., Nishimura, M., Matsumoto, G.I., Kawai, T., 2009. High-time resolution AMS ^{14}C data sets for Lake Baikal and Lake Hovsgol sediment cores: changes in radiocarbon age and sedimentation rates during the transition from the last glacial to the Holocene. Quat. Int. 205, 12–20.
Weninger, B., Jöris, O., Danzeglocke, U., 2007. CalPal-2007. Cologne radiocarbon calibration & palaeoclimate research package. http://www.calpal.de. (Accessed 20 June 2016).
Xiao, J., Si, B., Zhai, D., Itoh, S., Lomtatidze, Z., 2008. Hydrology of Dali Lake in central-eastern inner Mongolia and Holocene East Asian monsoon variability. J. Paleolimnol. 40, 519–528.
Xiao, J., Xu, Q., Nakamura, T., Yang, X., Liang, W., Inouchi, Y., 2004. Holocene vegetation variation in the Daihai Lake region of north-central China: a direct indication of the Asian monsoon climatic history. Quat. Sci. Rev. 23, 1669–1679.
Yang, X., Rost, K.T., Lehmkuhl, F., Dodson, J., 2004. The evolution of dry lands in northern China and in the Republic of Mongolia since the Last Glacial maximum. Quat. Int. 118/119, 69–85.
Yu, K., Lehmkuhl, F., Schlütz, F., Diekmann, B., Mischke, S., Grunert, J., Murad, W., Nottebaum, V., Stauch, G., 2016. Lake sediments documented late Quaternary humid pulses in Gobi Desert of Mongolia: vegetation, hydrologic and paleoglaciation implications. Geophys. Res. Abstr. 18. EGU 2016, 1894.
Yu, K., Lehmkuhl, F., Diekmann, B., Zeeden, C., Nottebaum, V., Stauch, G., 2017. Geochemical imprints of coupled paleoenvironmental and provenance change in the lacustrine sequence of Orog Nuur, Gobi Desert of Mongolia. J. Paleolimnol. https://doi.org/10.1007/s10933-017-0007-7.
Zhang, C., Zhang, W., Feng, Z., Mischke, S., Gao, X., Gao, D., Sun, F., 2012. Holocene hydrological and climatic change on the northern Mongolian Plateau based on multi-proxy records from Lake Gun Nuur. Palaeogeogr. Palaeoclimatol. Palaeoecol. 323–325, 75–86.